Reinstatement of *RIG-I* in chickens via genetic modification reveals new insights into the dynamic evolution of avian immune sensors

Hicham Sid[1*], Theresa von Heyl[1], Sabrina Schleibinger[1], Romina Klinger[1], Rodrigo Guabiraba[3], Vanaique Guillory[3], Benjamin Schade[4], Daniel Elleder[5], Samantha Sives[6], Lonneke Vervelde[6], Sascha Trapp[3], Benjamin Schusser[1,2]

[1] TUM School of Life Sciences, Weihenstephan, Department of Molecular Life Sciences, Reproductive Biotechnology, Technical University of Munich, 85354, Freising, Germany
[2] Center for Infection Prevention (ZIP), Technical University of Munich, 85354 Freising, Germany
[3] UMR ISP, INRAE, Université de Tours. 37380, Nouzilly, France.
[4] Bavarian Animal Health Service, Department of Pathology, 85586, Poing, Germany;
[5] Institute of Molecular Genetics of the Czech Academy of Sciences, Prague, Czech Republic
[6] Division of Immunology, The Roslin Institute and Royal (Dick), School of Veterinary Studies, University of Edinburgh, UK

[*]Correspondence: hicham.sid@tum.de

Graphical abstract

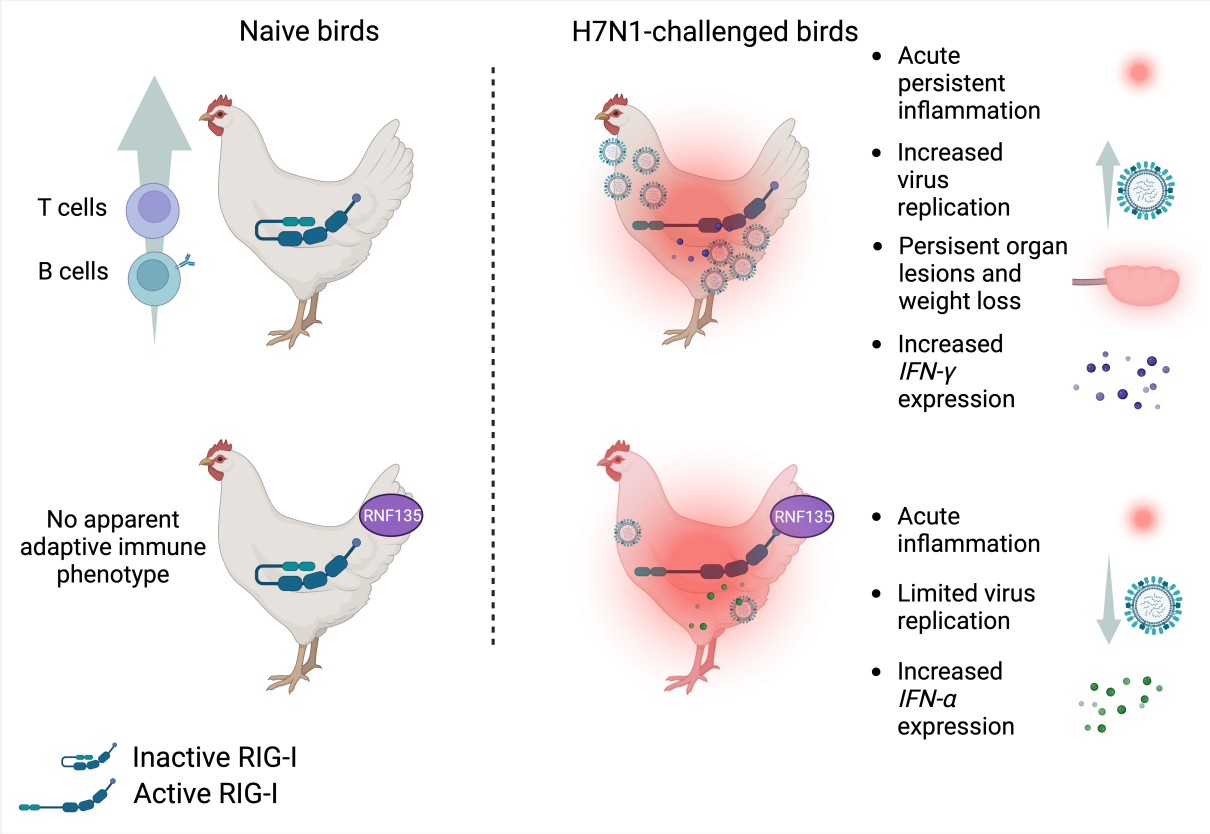

Abstract

Retinoic acid-inducible gene I (*RIG-I*) activates mitochondrial antiviral signaling proteins, initiating the antiviral response. *RIG-I* and *RNF135*, a ubiquitin ligase regulator, are missing in domestic chickens but conserved in mallard ducks. It was long believed that chickens' *RIG-I* loss was linked to increased avian influenza susceptibility. We reinstated both genes in chickens and examined their susceptibility to the avian influenza virus H7N1. Uninfected *RIG-I*-expressing chickens exhibited shifts in T and B cells, while the H7N1 infection led to severe disease, persistent weight loss, and increased viral replication. Conversely, the co-expression of *RIG-I* and *RNF135* reduced the viral replication and was associated with high inflammatory response. Our data indicate that the loss of *RIG-I* in chickens likely evolved to counteract deleterious inflammation caused by viral infection. We highlight the effects of restoring evolutionary lost genes in birds and suggest a new immunological approach to reduce viral replication and prevent infection.

69 **Introduction:**
70
71 Avian influenza virus (AIV) is an epizootic pathogen with zoonotic potential [1] that recently
72 caused devastating outbreaks worldwide, leading to the loss of more than 131 million birds due
73 to animal death and culling [2]. The viral reservoir of AIV are wild birds of the orders
74 *Anseriformes* (ducks, geese, and swans) and *Charadriiformes* (gulls and terns) [3], which,
75 compared to chickens or other galliform birds, exhibit milder clinical symptoms despite
76 efficient viral replication [4]. Certain genomic features of the duck, including a functional *retinoic*
77 *acid-inducible gene I (RIG-I)* gene, were reported to be associated with their relative resistance
78 to clinical avian influenza infection [5]. *RIG-I* is a cytosolic RNA sensor that recognizes and binds
79 to the 5' triphosphate end (5'-ppp) [6]. It forms a first line of antiviral defense as a pathogen
80 recognition receptor (PRR) against RNA viruses [7]. Upon activation, the *RIG-I* interacts with
81 the mitochondrial antiviral signaling proteins (MAVS), inducing a pro-inflammatory antiviral
82 response characterized by the upregulation of type I and type III interferons (IFNs) followed by
83 the expression of IFN stimulated genes (ISGs) [8]. The activity of *RIG-I* is believed to be
84 controlled by post-translational modification of *tripartite motif-containing protein 25*
85 (*TRIM25*) [9] and *RING finger protein 135* (*RNF135*, also known as *Riplet* or *REUL*). The latter
86 was found to modify *RIG-I* by lysine 63-linked polyubiquitination of the C-terminal region of
87 the *caspase activation and recruitment domain* (CARD) [10], leading to a stronger *RIG-I* signal
88 transduction [11]. The physiological role of mammalian *RIG-I*, its function in viral infections, and
89 its parallel evolution with other RLRs are well documented [9, 12, 13, 14]. Furthermore, the knockout
90 (KO) of *RIG-I* in mice has shown that this gene may have additional functions related to
91 adaptive immunity [12]. *RIG-I* KO mice exhibited a defect in migratory dendritic cells in
92 combination with a reduced frequency of polyfunctional effector T cells upon influenza
93 infection [15].
94 In ducks, *RIG-I* elicits a potent interferon (IFN) response within the first few hours after
95 infection, leading to survival against most AIV strains [16]. In contrast, chickens lack *RIG-I*,
96 which probably lost its function in a common ancestor of galliform birds [17, 18]. Interestingly, a
97 recent study detected disrupted *RIG-I* pseudogenes in some Galliformes, including the helmeted
98 guineafowl (*N. meleagris*) and the northern bobwhite (*C. virginianus*) [19]. Authors hypothesized
99 a compensatory evolution of *melanoma differentiation-associated gene-5* (*MDA5*) that
100 accompanied the gradual loss of *RIG-I* in chickens [19]. The evolutionary loss of *RIG-I* in different
101 galliform birds correlated with the simultaneous loss of its ubiquitin ligase *RNF135* [19], which
102 has been described to be critical for *RIG-I* ubiquitination in mammals, unlike *TRIM25*, which
103 is increasingly believed to be less important for *RIG-I* signaling [20]. Reasons behind the loss of
104 *RIG-I* and its ubiquitination factor in chickens are still unknown and remain enigmatic,

especially given the virus-limiting effect of duck *RIG-I* overexpression in AIV-infected chicken DF-1 cells [5].

To date, the effect of *in vivo* expression of *RIG-I* in chickens has never been studied, and no transgenic chicken lines expressing duck *RIG-I* have been generated, likely due to the lack of suitable biotechnological tools in avian research. Here, we used chicken primordial germ cells (PGCs) to develop genetically modified chickens expressing duck *RIG-I* and *RNF135* under the control of their respective duck promoters. The generated birds were healthy and developed normally compared to their WT siblings. In the absence of infection, we observed an alternative phenotype of the adaptive immune system of *RIG-I*-expressing chickens, particularly regarding the T cell population. In contrast, the co-expression of *RNF135* with *RIG-I* contributed to a balanced adaptive immune phenotype that appeared to be similar to WT birds. Infection experiments with an H7N1 AIV led to severe clinical disease associated with a strong inflammatory response, high *IFN-γ* expression, and elevated viral replication in *RIG-I*-expressing chickens compared to other challenged groups. In contrast, infected *RIG-I-RNF135*-expressing chickens presented with inflammation, limited viral replication, and increased *IFN-α* expression levels. The obtained data reveal the immunological functions of *RIG-I* in chickens and the benefit of learning from less susceptible species to influenza infection to improve the resilience of the immune system towards infection.

Results:

Generation of PGCs that express duck *RIG-I* and *RNF135* under the respective duck promoters

The genetic modification of PGCs represents a crucial step for generating transgenic chickens. PGCs are the precursors of sperm and eggs in adult animals, and therefore, we used them to produce chimeric roosters paired with WT layer hens to obtain the desirable transgene. To generate chickens that express *RIG-I* and *RNF135*, we started by cloning duck *RIG-I* and *RNF135*, which were subsequently inserted into two different expression vectors (Fig. 1A, 1B). *RIG-I* and *RNF135* were expressed under their respective duck promoters and used to generate PGCs expressing both genes separately. While the duck *RIG-I* promoter was previously described [21], we determined the activity of the duck *RNF135* promoter, which was examined by the generation of different deletion mutants tested in the NanoDLR™ Assay System. Therefore, different deletion mutants were generated, including p1577, p1001, p349, and p197. Since we did not detect a core promoter activity of the duck *RNF135*, we used the full-length sequence of the duck *RNF135* for the generation of duck *RNF135*-expressing PGCs (Fig. 1A). The assembled expression vectors that were used to generate PGCs are presented in Fig. 1B.

142 Due to the unavailability of commercial antibodies for detecting the duck *RIG-I*, we inserted a
143 FLAG-Tag on the C-terminus to facilitate its detection using anti-FLAG antibodies. The
144 activity of the duck *RIG-I* was examined by differentiating the *RIG-I*-expressing PGCs into
145 PGC-derived fibroblasts (Fig. 1C) that were infected with a low pathogenic avian influenza
146 virus (LPAIV) H9N2 (Fig. 1D). Results showed that the infection led to activation of *RIG-I* as
147 shown by FLAG-Tag staining. At the same time, the MOCK-infected cells remained negative
148 for *RIG-I* expression (Fig. 1D).
149
150 **The expression of *RIG-I* did not limit the viral replication under *in vitro* and *in ovo***
151 **conditions**
152 According to previously published data by Barber et al. [5], the overexpression of duck *RIG-I* in
153 chicken DF-1 cells reduced the replication of avian influenza viruses. Authors constitutively
154 expressed *RIG-I* under the control of the CMV promoter using expression vector pcDNA 3.1.
155 Therefore, we wanted to examine if the expression of *RIG-I* under the control of the duck RIG-
156 I promoter can lead to a similar effect in limiting virus replication. We isolated CEFs and
157 embryonated eggs obtained from the generated transgenic chickens and infected them with
158 LPAIV H9N2. After virus infection, supernatants and allantoic fluid were collected from CEFs
159 and embryonated eggs, respectively. We quantified the newly produced viral particles using a
160 focus-forming assay. Surprisingly, transgene expression did not significantly affect the viral
161 replication in both tested systems (Fig. 1D and 1E), which was the opposite in the previously
162 published study [5]. This highlights the importance of the chosen promoter, which may have
163 affected the expression of *RIG-I* and influenced the innate immune response towards the
164 influenza virus.
165
166 **Phenotypic characterization of the genetically modified chickens**
167 Upon the generation of *RIG-I*- and *RNF135*-expressing chicken lines, we wanted to ensure that
168 the genetic modification did not negatively affect the growth of the generated transgenic birds.
169 Therefore, we monitored their development by weekly measuring their body weights (Fig. 2A).
170 Both generated chicken lines showed comparable growth to their WT siblings. The animals
171 matured sexually, and no harmful phenotype was detected (Fig. 2A and 2B). The expression of
172 both genes was examined via RT-PCR, revealing that both genes are expressed differentially
173 in various tissues (Fig. 2C).
174 According to previously published studies, mammalian *RIG-I* affects adaptive immunity,
175 mainly T cells [15]. Therefore, we sought to examine whether the re-expression of *RIG-I* in
176 chickens will have similar effects. We analyzed the numbers of peripheral blood mononuclear
177 cells (PBMCs) using flow cytometry to investigate the possible impact of expressing *RIG-I*,

178 *RNF135,* or both on immune cell counts. No differences were observed in the number of
179 immune cells between *RNF135*-expressing chickens and their WT siblings (Supplementary file
180 1). However, *RIG-I*-expressing chickens exhibited a significantly higher number of αβ and γδ
181 T cells as well as B cells in comparison to their WT siblings ($p<0.05$) (Fig. 2D). This was not
182 the case for monocyte counts, where no significant differences were observed (Fig. 2D). In
183 addition, no significant differences were observed in *RIG-I*-expressing chickens compared to
184 WT birds regarding the levels of IgM and IgY at 12 and 14 weeks of age (Supplementary file
185 2).
186 Further analysis of different T cell subpopulations indicated that *RIG-I*-expressing chickens had
187 a significantly higher number of CD4+T cells and a significantly lower number of CD8α+T
188 cells ($p<0.05$) (Fig. 3). T-cell activation was quantified after lectin activation using
189 Concanavalin A (ConA). *RIG-I*-expressing chickens had a higher level of T cell activation in
190 TCRγδ/CD25+ T cells, which was not the case for TCRαβ1, αβ2/CD25+ T cells (Fig. 3).
191
192 Heterozygous birds expressing each gene separately were crossed to obtain birds that
193 simultaneously express both genes *RIG-I* and *RNF135*. The obtained *RIG-I-RNF135*-
194 expressing chickens were monitored weekly for weight gain and closely investigated at eight
195 and twelve weeks of age for possible alternate immune phenotypes similar to those observed in
196 *RIG-I*-expressing birds. Unlike *RIG-I*-expressing chickens, no significant differences in T cells
197 or B cell counts were detected in *RIG-I-RNF135*-expressing chickens in comparison to their
198 WT siblings (Fig. 4). This was also the case for body weight gain, where no significant
199 differences were observed in comparison to WT birds (Supplementary file 3).
200 These data indicate that the *RIG-I*, an innate immune sensor, can influence adaptive immunity
201 by causing shifts in T and B cell populations. In contrast, co-expression of *RNF135* with *RIG-*
202 *I* seems to balance the adaptive immune cell populations, which was comparable to WT birds.
203
204 ***RNF135* is required for efficient antiviral activity of *RIG-I***
205 The role of *RNF135* as an essential ubiquitination factor that supports the antiviral activity of
206 *RIG-I* was previously determined in mammalian cells [11]. Later on, *RNF135* was found to be the
207 obligatory ubiquitin for *RIG-I* [22], while so far, this was not known in birds. We investigated the
208 effect of expressing *RNF135* on the antiviral activity of *RIG-I* in genetically modified chickens.
209 We examined the susceptibility of the generated transgenic lines towards an H7N1 AIV, a direct
210 precursor of a highly pathogenic avian influenza virus (HPAIV), known to cause severe acute
211 respiratory disease in chickens [23]. Birds were challenged with the virus and monitored for
212 clinical signs, weight gain, viral replication, and lesion development. *RIG-I*-expressing
213 chickens had the highest rate of morbidity, as indicated in Fig. 5A. The clinical symptoms

214 started within the first two days of infection, where the morbidity rate reached a significant rate
215 of 44% at one-day post-infection (dpi) ($p<0.05$) and increased to 67% at two dpi ($p<0.05$),
216 which then decreased to 18% by three dpi ($p<0.05$). The onset of clinical disease was
217 accompanied by a significant weight loss at two dpi that remained significantly low at six dpi
218 ($p<0.05$) (Fig. 5C) and coincided with a pulmonary lesion score that increased from 0.8 at two
219 dpi to 2.3 at six dpi (Fig. 6A and 6B). This was also confirmed by histological assessment of
220 the caecum that revealed necrotic lesions associated with pronounced epithelial hyperplasia
221 (Fig. 6B). *RIG-I-RNF135*-expressing chickens exhibited increasing clinical illness, from 13%
222 of sick animals at one dpi to 50% at three dpi ($p<0.05$). Severe clinical symptoms associated
223 with mortality in this group lasted until six dpi.
224 The expression of *RNF135* alone resulted in a mortality rate comparable to WT birds. In
225 contrast, the clinical symptoms in *RNF135*-expressing chickens lasted till three dpi with a total
226 of 25% sick animals (Fig. 5). This was not the case for WT chickens that exhibited clinical
227 symptoms only for the first two days after infection and had a morbidity rate of 13% and 19%
228 at one and two dpi, respectively (Fig. 5).
229 The quantification of the virus genome copies via qRT-PCR showed that the expression of *RIG-*
230 *I* together with *RNF135* resulted in an efficient antiviral effect, as demonstrated by the lowest
231 amount of viral genome copies in the caecum compared to all the other challenged chicken lines
232 (Fig. 5D), with a significant low viral replication rate compared to *RIG-I* expressing chickens
233 at two and six dpi ($p<0.05$). In the lung, challenged *RIG-I-RNF135*-expressing chickens
234 displayed a virus replication rate similar to WT birds and a significantly lower replication rate
235 than *RIG-I*-expressing chickens at two dpi ($p<0.05$). Conversely, *RIG-I*-expressing chickens
236 had the highest viral replication rate in the lung and the caecum among all investigated groups,
237 with a significant difference compared to *RIG-I-RNF-135*-expressing chickens ($p<0.05$) (Fig.
238 5D). The amount of viral nucleic acid remained at a high level at six dpi, indicating the lack of
239 viral clearance in these birds, which was not the case for the other challenged chicken lines
240 (Fig. 5D).
241 The observed low viral titer in *RIG-I-RNF135*-expressing chickens confirms the crucial role of
242 *RNF135* as a ubiquitin ligase at the early stage of infection. Also, it demonstrates that the
243 chicken *TRIM25* does not overtake the part of *RNF135* in *RIG-I*-expressing chickens.
244
245 **The expression of *RIG-I* and *RNF135* in H7N1-challenged birds coincided with the acute**
246 **phase of infection.**
247 We aimed to quantify possible changes in the expression levels of both transgenes in the
248 challenged animals after the H7N1 infection. We quantified *RIG-I* and *RNF135* expressions via
249 qRT-PCR in the lung, and the caecum (Fig. 5E). The caecal expression of *RIG-I* in virus-

250 infected *RIG-I-RNF135* chickens was increased by ~26 folds. At the same time, infected *RIG-*
251 *I* chickens exhibited an increase of ~24-fold compared to *RIG-I-RNF135* MOCK controls.
252 Infected *RIG-* and *RIG-RNF135*-expressing chickens had a comparable *RIG-I* expression to
253 *RIG-RNF135*-MOCK controls with no significant upregulation (Fig. 5E). Overall, we observed
254 lower expression of *RNF135* in the caecum and lungs compared to *RIG-I-RNF135*-MOCK
255 controls. The expression increased by 1.4 folds in *RNF135*-infected birds and ~2 folds in *RIG-*
256 *I-RNF135*-infected chickens. In the lung, the *RNF135* expression at two dpi was upregulated
257 by ~6 folds and ~4 folds in infected *RIG-I* and *RIG-I-RNF135*-expressing chickens,
258 respectively. At six dpi, the *RNF135* expression was at a comparable level with the *RIG-I-*
259 *RNF135* MOCK controls (Fig. 5E). These data indicate that the infection led to a quick
260 upregulation of *RIG-I* at the acute phase of infection, which quickly decreased afterward.
261

262 **Differential regulation of innate immune genes in naïve as well as in H7N1-challenged**
263 ***RIG-I*, *RNF135,* and *RIG-I-RNF135*-expressing chickens**

264 We speculated that the observed acute inflammatory reaction could be due to a differential
265 regulation of inflammatory genes related to *RIG-I* signaling. Therefore, we sought to quantify
266 the differentially expressed genes (DEGs) between transgenic and WT birds. We used the
267 Fluidigm qRT-PCR array to identify changes in the expression of selected innate immune genes
268 in both naïve and H7N1-challenged birds [24]. The results revealed that in the absence of
269 infection, *RIG-I-RNF135*-expressing chickens already had a significantly higher expression of
270 ISGs in the caecum, including *ISG12-2* and *OASL,* as well as the transcription factor *EGR1*. In
271 contrast, others, including *EGR1*, *IL41*, *Il1β,* and *IL8,* were significantly upregulated in the
272 spleen (Fig. 7 and Supplementary file 4).
273 The comparison of challenged groups with non-infected controls (WT-MOCK) indicated that
274 *RIG-I* chickens expressed several inflammatory genes in the caecum and lungs that were not
275 expressed in the other groups. This included *IFITM1*, *IL6,* and *LIPI* (Fig. 7 and Supplementary
276 file 4). At two dpi, we observed the upregulation of genes involved in the JAK-STAT signaling
277 pathway, including *IL-6* and *STAT3*. The significant upregulation of inflammatory and immune
278 regulatory genes in the *RIG-I*-expressing chickens persisted until six dpi, where over 20 genes
279 were exclusively upregulated in the spleen (Fig. 7 and Supplementary file 4). This was not the
280 case for *RIG-I-RNF135*-expressing chickens and WT chickens with an exclusive expression of
281 three and seven genes, respectively (Fig. 7 and Supplementary file 4). In addition, the analysis
282 of expressed genes in the spleen revealed that only *RIG-I-RNF135* chickens expressed *IRF7*
283 and *TRIM25*, which was not the case for *RIG-I* chickens (Fig. 7 and Supplementary file 4).
284 The functional enrichment analysis of the genes involved in the biological processes of
285 transgenic chickens indicated that the regulated genes in *RIG-I*-expressing chickens were highly

286 involved in metabolic activities. In contrast, those in *RIG-I-RNF135*-expressing birds were
287 primarily involved in regulatory mechanisms (Supplementary file 5). Overall, the obtained data
288 confirm that *RIG-I*-expressing chickens exhibited a significant increase of inflammatory
289 cytokines that were not observed in other challenged birds, which may explain the acute
290 inflammatory reaction in these birds.
291
292 **High expression of *IFN-γ* is associated with significant virus replication in *RIG-I*-**
293 **expressing birds**
294 Since we observed a significant reduction of viral genome copies in the *RIG-I-RNF135*-
295 expressing chickens compared to *RIG-I*-expressing birds, we compared the DEGs between
296 H7N1-infected groups. This helped us determine possible factors behind the increased H7N1
297 replication in *RIG-I*-expressing birds. Interestingly, these birds lacked interferon upregulation
298 compared to infected WT birds or *RIG-I-RNF135*-expressing chickens. We also found that the
299 viral infection led to a significant increase in the expression of *IFN-γ* at six dpi when compared
300 to H7N1-infected *RIG-I-RNF135*-expressing chickens (14-fold change increase) and WT birds
301 (9-fold change increase) (Fig. 8) ($p<0.05$). In contrast, *RIG-I-RNF135*-expressing birds quickly
302 exhibited a significant increase of *IFN-α* expression, already at two dpi, in comparison to *RIG-*
303 *I*-expressing birds (12-fold change) as well as to WT birds (17-fold change) (Fig. 8). We
304 concluded that the co-expression of *RNF135* and *RIG-I* in chickens leads to a significant
305 increase of *IFN-α* expression, which was not observed when *RIG-I* was expressed solely. In
306 addition, *RIG-I*-expression caused an upregulation of *IFN-γ* that was accompanied by a
307 significant increase in virus genome copies.
308 **Discussion:**
309 The constant arms race between pathogens and the host affects different aspects of the immune
310 system, including innate sensors. The reason for the loss of *RIG-I* in Galliformes, which
311 correlated with the disappearance of the ubiquitin ligase *RNF135*, remained a mystery [19],
312 especially given the established contributing role of *RIG-I* in the resilience towards influenza
313 in ducks and other species [5, 25]. It was previously speculated that the gradual loss of *RIG-I* and
314 *RNF135* in the chicken was possibly caused by the pathogen's resistance to the innate sensor
315 or the disappearance of some relevant pathogens [19]. At the same time, preservation of the
316 antiviral competence accompanied the loss of *RIG-I* and *RNF135* in chickens via the
317 evolutionary selection of *MDA5* and *LGP2* [26]. The beneficial effect of the duck *RIG-I*-
318 overexpression in chicken DF-1 cells was demonstrated by the limited replication of AIV in
319 these transgene-expressing cells [5]. So far, no chickens expressing the duck *RIG-I* have been
320 generated to investigate their antiviral response *in vivo*. In this study, we produced genetically
321 modified chickens that express *RIG-I* with or without its ubiquitin ligase *RNF135* to examine

322 the physiological role of both genes and their function during AIV infection. Both genes were
323 cloned from the duck as it represents the most studied avian influenza reservoir with
324 evolutionary conserved *RIG-I* and *RNF135* [4, 19, 27]. The expression of both genes was controlled
325 under their respective duck promoters since the duck *RIG-I* was previously tested in chicken
326 cells (12). This strategy allows the strict control of gene expression that can be induced only
327 upon infection, which prevents undesirable production of inflammatory cytokines that may
328 cause autoimmune diseases [21]. While the duck *RIG-I* promoter was previously identified [21], we
329 described the activity of the duck *RNF135* promoter using chicken cells.
330 Without infection, *RIG-I* expression did not cause any harmful phenotype, but it led to different
331 adaptive immune cell counts compared to WT siblings. We observed that, unlike CD4+ T cells,
332 *RIG-I*-expressing chickens had a significantly lower number of CD8α+ T cells than WT-
333 chickens, which can be comparable to mice where *RIG-I* signaling limits the number of $CD8^+$
334 T cells [28]. This suggests the role of the *RIG-I* in priming T cell immunity in the chicken, which
335 can be similar to mice that exhibited a lack of T cell immunity associated with deficiencies in
336 migratory dendritic cell activation and viral antigen presentation [15 12]. The effect of *RIG-I* on
337 adaptive immunity was further confirmed by others who reported defects in CD8+ and CD4+
338 T cells priming after *RIG-I* KO [29].
339 Conversely, *RIG-I-RNF135*-expressing chickens appeared to have a balanced adaptive immune
340 profile indistinguishable from WT birds. This observation demonstrates the possible role of
341 *RNF135* in modulating the T cell immune response in birds, which was previously described
342 for Th1 response and cytotoxic T cells in mice [30]. Moreover, naïve *RIG-I-RNF135*-expressing
343 chickens had a significantly higher expression of *interleukin 4 inducible gene 1* (*IL4I1*) as well
344 as *protein nuclear translocation 7 (IRF7*) and *tripartite motif-containing protein 29 (TRIM29)*.
345 This may explain the differential adaptive immune phenotype between *RIG-I* and *RIG-I-*
346 *RNF135*-expressing chickens. Previous studies indicated the involvement of *IL4I1* in the
347 signaling to T and B lymphocytes [31] and the effective role of translocation factors such as *IRF7*
348 in chicken cells transfected with the duck *RIG-I* [21].
349 The lack of an antiviral effect after *in ovo* and *in vitro* experimental infections with LPAIV
350 H9N2 was discordant with the previously described antiviral effect of duck *RIG-I* in chicken
351 DF-1 cells [5]. Barber et al, observed low virus replication upon the overexpression of *RIG-I*
352 under control of the CMV promoter. The difference between our results and previously
353 published data can be related to the chosen promoter used by Barber et al, which may lead to a
354 higher upregulation of *RIG-I* and, consequently, a strong production of interferon-stimulated
355 genes.
356 H7N1-challenge experiments of the generated transgenic birds revealed that *RIG-I*-expressing
357 chickens had an early upregulation of proinflammatory cytokines such as *IL-6*, known to

support *IL1β* in suppressing regulatory T cells, which can lead to an uncontrolled increase in the number of CD4+ T cells [32]. Furthermore, the expression of *RIG-I* without *RNF135* was not beneficial in limiting H7N1 replication since the *RIG-I*-expressing chickens had the highest viral genome copies among all challenged groups. The requirement of *RNF135* for an efficient *RIG-I*-mediated antiviral effect was demonstrated by the significantly lower number of viral genome copies detected in *RIG-I-RNF135*-expressing chickens compared to *RIG-I*-expressing chickens, which was also previously described in mammalian cells [11]. In addition, we found that the H7N1 infection caused a significant upregulation of *RIG-I* in the caecum compared to the lungs. This can be because *RIG-I* expression rapidly takes place upon stimulation and may reach a peak by three hours post-infection [33]. Similar observations were described by Cornelissen et al. that detected a significant upregulation of *RIG-I* expression in lungs of ducks at 8h post H7N1 infection that significantly decreased at two dpi [34]. Infected *RIG-I*-expressing birds exhibited an acute inflammatory response and weight loss at two dpi that lasted till six dpi. Pang et al, reported that the inflammatory reaction associated with *RIG-I* signaling could be used by the influenza virus for its replicative advantage, particularly in the respiratory tract [13]. *RIG-I*-expressing birds showed several regulated immune genes compared to other infected groups, including upregulation of the *suppressor of cytokine signaling 1* (*SOC1*) in the caecum. This may explain the significant increase in viral genome copies and the observed T cell phenotype since *SOCS1* is a potent inhibitor of JAK/STAT signaling [35] and is involved in several mechanisms that regulate the T cell maturation, differentiation and function [36].
Interestingly, we detected significant upregulation of *IFN-γ* in the lungs of infected *RIG-I*-expressing chickens compared to infected *RIG-I-RNF135*- and WT-chickens, which can be responsible for lung-mediated injury and acute death caused by respiratory distress. The role of *IFN-γ* was previously described in *IFN-γ* KO mice that were less susceptible to lung inflammation and pathology upon influenza infection [37]. The lack of an antiviral effect in *RIG-I*-expressing chickens may also indicate that chicken *TRIM25* is dispensable for *RIG-I* efficient ubiquitination. Similar findings were described using human lung adenocarcinoma epithelial cells, where *TRIM25* did not participate in the endogenous *RIG-I*-dependent antiviral responses [20]. However, other studies done in mammalian models indicated that the deletion of *TRIM25* increases the susceptibility to influenza infection [38], supporting the evidence that *TRIM25* may bind directly to the viral RNA, thereby contributing to the restriction of influenza virus infection [39].

The low viral replication in *RIG-I-RNF135*-expressing chickens can be related to the effectiveness of *RNF135* in *RIG-I*-mediated antiviral activity. This was reflected by the upregulation of *IFN-α* expression in infected birds on one side and the absence of

394 immunophenotype in naïve birds on the other side, suggesting a stabilizing role of *RNF135* that
395 can be comparable to the role *TRIM25* [40]; however, this requires further investigations. *RIG-I-*
396 *RNF135*-expressing chickens also exhibited an acute upregulation of *early growth response 1*
397 (*EGR1*). This transcription factor participates in several functions, including cell death and the
398 induction of a large repertoire of inflammatory genes [41]. This was supported by the histological
399 assessment that revealed the presence of multiple necrotic cells in the caecum of *RIG-I-*
400 *RNF135*-expressing chickens. Overall, the increased death in *RIG-I-RNF-135*-expressing
401 chickens, which was beneficial in terms of antiviral effect, was deleterious for the birds due to
402 increased gene regulation and excessive immune response. Furthermore, the assessment of the
403 immunophenotype of *RNF135*-expressing chickens revealed that this gene, on its own, may
404 function independently from the *RIG-I* [42].
405 Our data suggest that the evolutionary loss of *RIG-I* in chickens and other galliform birds was
406 advantageous in coping with viral infections caused by AIV or other avian RNA viruses. This
407 subsequently helped decrease the acute inflammation and the damage to the host. A comparable
408 hypothesis was made in the case of pangolins that lost the *MDA5* as an evolutionary mechanism
409 to cope with coronavirus-induced inflammation [43]. Above that, we propose that the antiviral
410 role of *RIG-I* in ducks [5] is not exclusively related to this gene. Still, it may involve the
411 ubiquitination factor *RNF135* and possibly other unknown regulatory factors that support *RIG-*
412 *I* signaling and reduce the repercussions of acute inflammation by negatively regulating the
413 *RIG-I* signaling [44]. We provided novel information regarding the outcome of the re-introduction
414 of *RIG-I* and its ubiquitination factor *RNF135* in the chicken genome. Future work should focus
415 on identifying factors that can help reduce the acute inflammatory reaction in *RIG-I-RNF135-*
416 expressing chickens while maintaining potent antiviral activity, which can lead to the
417 generation of avian influenza virus-resistant chickens.
418
419 **Materials and Methods**
420 **Cloning of the duck *RIG-I* and the duck *RIG-I* promoter**
421 Total RNA was isolated from the spleen of the mallard duck (*Anas platyrhynchos*) using
422 ReliaPrep™ RNA Tissue Miniprep System (Promega, USA), followed by cDNA synthesis
423 using GoScript™ Reverse Transcription System (Promega, USA) according to the
424 manufacturer's instructions. The duck *RIG-I* was amplified using Q5® High-Fidelity DNA
425 Polymerase (New England Biolabs, USA) using the primers 562_RIG-I_for (5'-
426 ATGACGGCGGACGAGAAGCGGAGC-3') and 563_RIG-I_rev (5'-
427 CTAAAATGGTGGGTACAAGTTGGAC-3') that were previously described [45]. The PCR
428 thermal conditions were as follows: 98 °C 30 sec, followed by 35 cycles of 98 °C 10 sec, 67 °C
429 20 sec, 72 °C 1:30 min, and a final extension step of 72 °C 2 min.

430 The entire length of the duck *RIG-I* promoter was amplified using primers 706_RIG-I_For (5'-
431 AGCTGATGACCTGCAAAAAGTT-3') and 661_RIG-I_Rev (5'-
432 GGCTGGGCTCTGCCGGCCG-3'), which were described elsewhere [21]. This resulted in an
433 amplicon of 2017 bp that was fully sequenced and aligned with the duck genome (*Anas*
434 *platyrhynchos*, NC_040075.1). The PCR was conducted following the following thermal
435 conditions 98 °C 30 sec, followed by 35 cycles of 98 °C 10 sec, 70 °C 20 sec, 72 °C 1:30 min,
436 and a final extension step of 72 °C 2 min.

437 **Cloning of the duck *RNF135***

438 The genomic region containing duck *RNF135* was obtained from the GenBank contig
439 PEDO01000017.1 and corrected based on multiple publicly available duck RNAseq data.
440 Although the *RNF135* sequence was correctly predicted in many birds, we detected a partially
441 incomplete annotated sequence of the duck *RNF135*, specifically the missing 5' part that
442 contains the RING domain (previous accession number XM_013092775), while the predicted
443 version of the *RNF135* was made available (XM_027471415.2). The full-length sequence of
444 the duck *RNF135* was synthesized after codon optimization using the IDT online tool (IDT™,
445 USA) (Supplementary file 6). The obtained *RNF135* sequence was subsequently cloned into
446 the *RNF135*-expression vector driven by the duck *RNF135* promoter (Fig. 1B).

447 **Identification of the duck *RNF135* promoter via Nano-Glo® Dual-Luciferase® Reporter**
448 **Assay**

449 The potential duck *RNF135* promoter was obtained by amplifying 1577 bp 5' of the ATG start
450 codon from the gDNA of duck that was cloned into pGEM vector (Promega, USA) and
451 analyzed by Sanger sequencing. The PCR was done using Q5® High-Fidelity DNA Polymerase
452 with primers: 707_RNF_Prom_For (5'-GA GCA GAG CCA GGC AGC TAT A-3'), 708 (5'-
453 GGT CCT GCT CGG GGC GGA GC-3') resulting in an amplicon of 1557 bp. The PCR
454 thermal conditions were conducted using Q5® High-Fidelity DNA Polymerase (New England
455 Biolabs, USA) at two step-PCR 98 °C 30 sec, 98 °C 10 sec, 72 °C 60 sec and a final elongation
456 step of 72 °C 2 min.

457 The promoter activity of the duck *RNF135* was assessed by measuring promoter-driven
458 NanoLuc™ luciferase activity normalized to the luminescence of Firefly luciferase. To this
459 end, a total of 50.000 chicken DF-1 cells were seeded in 24 well plates and were co-transfected
460 24h later with a vector plasmid containing the deletion mutant and a second plasmid for the
461 expression of Firefly under the PGK promoter (Promega, USA). 24h after transfection, cells
462 were washed with PBS, trypsinized, and resuspended in 250µl culture medium. Firefly signal
463 was detected by mixing 80µl of the cell suspension with the same amount of ONE-Glo™ EX
464 Reagent, prepared by combining ONE-Glo™ EX Luciferase Assay Buffer with ONE-Glo™
465 EX Luciferase Assay Substrate in 1:1 ratio (Promega, USA). After measuring the signal of the

466 Firefly luciferase in the GloMax® 20/20 Luminometer (Promega, USA), 80 µl NanoDLR™
467 Stop & Glo® reagent, prepared by adding NanoDLR™ Stop & Glo® Substrate 1:100 into
468 NanoDLR™ Stop & Glo® Buffer (Promega, USA), were added to the samples. These were
469 incubated for 10, 30, 60, and 120 min and measured again in the GloMax® 20/20 Luminometer
470 (Promega, USA) to detect the NanoLuc™ Luciferase. The cell-free culture medium was used
471 as a blank control.

472 **Determination of the Transgene Copy Number by Droplet Digital PCR**

473 Droplet digital PCR (ddPCR) was used to select PGC clones with a single genomic transgene
474 integration and was performed as described previously with slight modifications [46]. Briefly,
475 500ng of gDNA was digested with 20 units XbaI (New England Biolabs, Germany) for one h,
476 followed by an inactivation step at 65°C for 20 min. The Taqman PCR reaction was set up
477 using 10ng digested DNA, 2× ddPCR supermix for probes (no dUTP) final concentration 1×
478 (Bio-Rad Laboratories, USA), a 20× target primer/FAM-labeled probe mix, and a 20× reference
479 primer/HEX-labeled probe mix, which was followed by droplet generation using the QX200
480 Droplet Generator by mixing 20ul of the TaqMan PCR reaction with 70ul droplet generator oil
481 in a DG8 Cartridge. The cycling conditions comprised a 95°C for 10min, followed by 40 cycles
482 of 94°C for 30 sec, 59°C for 60 sec, and a final hold for 98°C for 10 min with a 2°C/s ramp rate
483 at all steps. The copy number was determined by calculating the proportion of positive and
484 negative droplets using a QX200 droplet reader, which was then analyzed using Quantasoft
485 software (Bio-Rad Laboratories, USA) (Supplementary file 7). The hygromycin fluorescent
486 labeled-probe ([5′FAM-TCGTGCACGCGGATTTCGGCTCCAA-3′] along with the primers:
487 ddHygro_F [5′-CATATGGCGCGATTGCTGATC-3′] and ddHygro_R [5′-
488 GTCAATGACCGCTGTTATGC-3′]). As a reference gene, we used the beta-actin probe
489 ([5′HEX-GTGGGTGGAGGAGGCTGAGC-BHQ3′] along with the primer combination
490 ddBeta_actin_F: [5′-CAGGATGCAGAAGGAGATCA-3′] and ddBeta_actin_R: [5′-TCCACC
491 ACTAAGACAAAGCA- 3′]). The quantification was done using the QX100 system (Bio-Rad
492 Laboratories, USA) (Supplementary file 7).

493 **Stimulation of duck *RIG-I* expression in PGC-derived fibroblasts**

494 The generated *RIG-I*-expressing PGCs were differentiated into fibroblasts (PGCFs) as
495 previously described [47] and subsequently infected with a LPAIV H9N2 to examine the ability
496 of *RIG-I* to detect its ligand. Briefly, 50.000 cells were seeded into 48 well plates and infected
497 with an MOI of 0.1 for 18h before they were fixed and stained using immunofluorescence, as
498 previously described [48]. Cells were fixed with 4% PFA and kept on ice for 10 min.
499 Subsequently, they were washed with PBS and permeabilized with 0.5% Triton X. The FLAG-
500 Tag was detected by using a mouse anti-FLAG antibody (Supplementary file 8) that was
501 incubated for 1h, followed by staining with goat anti-mouse Alexa 568 (Supplementary file 8).

502 Slides were subsequently covered with a mounting medium that contains DAPI for staining the
503 nucleus and covered with coverslips (Vector Laboratories, Inc., USA). Fluorescence
504 microscopy was performed with a fluorescence microscope (ApoTome, Zeiss).

505 **Generation of *RIG-I*-and *RNF135*-expressing chickens**

506 White Leghorns (Lohmann selected White Leghorn (LSL), Lohmann-Tierzucht GmbH,
507 Cuxhaven, Germany) were used to generate transgenic chicken lines. Animal experiments were
508 approved by the government of Upper Bavaria, Germany (ROB-55.2-2532.Vet_02-18-9).
509 Experiments were performed according to the German Welfare Act and the European Union
510 Normative for Care and Use of Experimental Animals. All animals received a commercial
511 standard diet and water *ad libitum*. PGCs that express either *RIG-I* or *RNF135* were generated
512 using the DNA constructs shown in Fig. 1, as previously described [49, 50]. To ensure the stable
513 integration of the transgene, we used the phiC31 integrase-mediated integration [51]. Briefly, LSL
514 PGCs were derived from the blood of male embryonic vasculature at stages 13-15, according
515 to Hamburger and Hamilton [52]. They were cultured at 37°C in a 5% CO2 environment using
516 modified KO-DMEM as described previously [53]. A total of $5x10^6$ cells per transgene were
517 washed with phosphate-buffered saline (PBS) and resuspended in 100µl Nucleofector™
518 Solution V (Lonza, Germany) containing the expression vector (Fig. 1B) and the integrase
519 expression construct. Electroporation was performed using an ECM 830 Square Wave
520 Electroporation System (BTX, USA), applying eight square wave pulses (350V, 100µsec).
521 After clonal selection using puromycin for *RIG-I* and blasticidin for *RNF135*, PGCs were
522 genotyped and tested for clones with one single genomic integration, which were then used to
523 generate the chimeric roosters. A total of 3000 cells with the desired genetic modification were
524 injected into the vasculature of 65h old embryos, transferred into a surrogate eggshell, and
525 incubated until the hatch. Upon sexual maturity, sperm was collected from chimeric roosters
526 for genotyping. [50, 54]. The germline-positive roosters were bred with wild-type hens to obtain
527 heterozygous animals (the germline transmission rate is presented in Supplementary File 9).
528 The examination of the inheritance of duck *RIG-I* and the genotyping of the offspring was done
529 via PCR using FIREPol DNA Polymerase (Solis Biodyne) using the primer combination
530 613_RIG-I-for (5'-CCTAGGAGAAGCATTCAAGGAG-3') and 563_RIG-I_Rev (5'-
531 CTAAAATGGTGGGTACAAGTTGGAC-3'). The following PCR conditions were used:
532 initial denaturation at 98 °C 30 sec, followed by 40 cycles of 98 °C 10 sec, 60 °C 30 sec, 72 °C
533 30 sec, and a final extension step of 72 °C 2 min, resulting in a fragment of 298bp. The
534 inheritance of the duck *RNF135* was examined using the primers combination 1121_RNF_For
535 (5'GCATGGGATCAACCGACAGCATC-3') and 1017_RNF_rev
536 (5'CCACACACCAACTTGACTCGGTC-3', using the following PCR conditions 98 °C 30

537 sec, followed by 40 cycles of 98 °C 10 sec, 60 °C 30 sec, 72 °C for 1 min and a final extension
538 step of 72 °C 2 min, resulting in an amplicon of 931bp.
539 Following the generation of different transgenic lines, they were monitored till sexual maturity
540 for possible harmful phenotypes that could been reflected in weight gain or the ability to
541 produce sperm or eggs. In addition, the immunophenotype of the generated birds was assessed
542 at 2, 5, 8, and 12 weeks after hatch by flow cytometry.

543 **Isolation, culture, and infection of chicken embryonic fibroblasts (CEFs)**

544 CEFs were isolated from 10-day-old (ED10) embryos according to the protocol published
545 elsewhere [55]. Before the isolation of CEFs, embryos were genotyped by collecting blood at
546 ED10 and preparing a window of 0.5 cm^2 in the eggshell that allowed access to the embryonic
547 vasculature. CEFs were cultured using Iscove's liquid medium containing stable glutamine
548 (Biochrom, Germany) that was supplemented with 5% fetal bovine serum (FBS) Superior
549 (Biochrom, Germany), 2% chicken serum (ThermoFisher Scientific, USA) and 1% Penicillin-
550 Streptomycin-Solution (Penicillin 10,000 U/ml and Streptomycin 10 mg/ml) (Biochrom.
551 Germany). Subsequently, CEFs were incubated at 40°C in a 5% CO2 atmosphere until
552 infection. The *in vitro* infection of CEFs with H9N2 was done after overnight seeding 250.000
553 cells/well in 6 well plates and infecting them in three independent experiments with
554 multiplicities of infection (MOIs) of 0.1 and 1. Supernatants were collected 24h post-infection
555 from the infected cells and titrated on MDCK (kindly provided by Prof. Silke Rautenschlein,
556 University of Veterinary Medicine, Hannover). The virus titration was done as previously
557 described [48].

558 ***In ovo* infection of embryonated eggs**

559 Fertilized eggs from a crossing of *RIG-I* (+/-) and *RNF135*(+/-) were collected and incubated
560 till ED10. Eggs were blindly infected with 10^3 FFU of LPAIV H9N2, as previously described
561 [56]. 24h post-infection, the allantois fluid and muscle tissue were collected respectively for viral
562 titration and genotyping. The virus titration was done on MDCK cells as previously described
563 [48].

564 **RT-PCR for the detection of transgene expression in different tissues**

565 RNA from chicken organs, including lung, trachea, heart, liver, duodenum, thymus, bursa, and
566 brain, was isolated with Reliaprep RNA Tissue Miniprep System according to manufacturer
567 instructions (Promega), followed by cDNA synthesis using GoScript Reverse transcription mix
568 (Promega). The detection of *RIG-I*, as well as *RNF135* from various tissues, was done using
569 the following primers. *RIG-I*: 613_RIG-I-for (5'-CCTAGGAGAAGCATTCAAGGAG-3')
570 and 563_RIG-I_Rev 5'-(CTAAAATGGTGGGTACAAGTTGGAC-3'), while *RNF135* was
571 detected using the following primers: 898_duRNF_for (5'-
572 CTTGAGAGAGGTGGAGGGAGC-3') and 899_duRNF_rev (5'-

573 GGGCTGGTGGGAATTGTTGAGG-3'). *RIG-I* and *RNF135* PCRs produced an amplicon of
574 298bp and 148bp, respectively. β-actin mRNA was detected with primers Beta_actin_F (5′-
575 TACCACAATGTACCCTGGC-3′) and Beta_actin_R (5′-CTCGTCTTGTTTTATGCGC-3′)
576 [57], resulting in a 300-bp amplicon. The PCR was performed using FIREPol DNA Polymerase
577 (Solis Bio-dyne) according to the manufacturer's instructions. The following PCR conditions
578 were used: initial denaturation at 98 °C 30 sec, followed by 40 cycles of 98 °C 10 sec, 59 °C
579 30 sec, 72 °C 30 sec, and a final extension step of 72 °C 2 min.

580 **Enzyme-linked immunosorbent assay (ELISA)**

581 ELISA was done to measure the total plasma IgM and IgY concentrations. Briefly, 96 well
582 plates were coated overnight with anti-chicken antibodies IgM and IgY at a concentration of
583 2µg/mL (Supplementary file 8). The next day, plates were washed three times with washing
584 buffer, followed by a blocking step with 4% skim milk for one hour. The prediluted plasma
585 samples in 1:3 serial dilution were pipetted in the plates and incubated for one hour. The
586 detection was done by using secondary HRP-conjugated antibodies at the concentrations
587 mentioned in Tabe1, which were incubated for 1h at RT. This was followed by adding
588 100µl/well of TMB (3,3', 5,5;-tetramethylbenzidine) substrate solution for 10 min, which was
589 stopped by 50µl per well of 1M sulfuric acid solution. The optical density (OD) was measured
590 using FluoStar Omega via the measuring filter 450nm and the reference filter 620 nm (Version
591 5.70 R2 BMG LABTECH, Ortenberg, Germany).

592 **Flow Cytometry**

593 Peripheral blood mononuclear cells (PBMCs) were isolated using Histopaque®-1077 density
594 gradient centrifugation (Sigma, Taufkirchen, Germany) and analyzed using flow cytometry.
595 Extracellular staining was carried out to detect various chicken immune cell markers including
596 T cell subpopulations, B cells and Monocytes (list of antibodies is mentioned in Supplementary
597 file 8). Briefly, $5x10^6$ cells were washed with 2% BSA diluted in PBS (FLUO-Buffer). To
598 determine the living cell population, cells were incubated with Fixable Viability Dye eFluor
599 780 (eBioscience, Thermo Fisher Scientific, USA). After washing with FLUO-Buffer, primary
600 antibodies (concentration shown in Table 2) were applied for 20 min. Cells were washed in
601 FLUO-Buffer to remove unbound antibodies and incubated with conjugated secondary
602 antibodies for 20 min. Subsequently, cells were again washed and analyzed using an Attune
603 flow cytometer (Thermo Fisher Scientific, USA). The obtained data were then analyzed with
604 FlowJo 10.8.1 software (FlowJo, Ashland, USA). An example of the gating strategy used in
605 this study is presented in supplementary file 10.

606 **Assessment of *in vitro* T cell activation**

607 PBMCs were isolated from 12 weeks old *RIG-I* or WT birds and resuspended in RPMI medium
608 supplemented with 10%FBS and 1% Penicillin/Streptomycin and distributed on a 48 well plate

609 with a total of $5x10^6$ cells/well. Cells were subsequently stimulated with Concanavalin A (Con
610 A) (eBioscience™) at a concentration of 25 µg per well. They were monitored every 24h for T
611 cell activation via flow cytometry. Activated T cells were stained for surface expression of
612 γδTCR1, CD25, or αβTCR2&3 using antibodies listed in Supplementary file 8.

613 **Challenge infection experiment with H7N1**

614 The challenge infection experiment was performed at the INRAE-PFIE platform (INRAE
615 Centre Val de Loire, Nouzilly, France) and approved by the local Ethics Committee Val de
616 Loire and the Ministère de l'Enseignement Supérieur et de la Recherche under the number
617 2021120115599580. Transgenic birds required for the experiment were hatched in dedicated
618 hatching isolators and genotyped by PCR using DNA extracted from EDTA blood samples
619 collected at day 7 post hatch. At 3 weeks of age, transgenic and WT-chickens were distributed
620 into four different groups (Supplementary file 11) corresponding to four BSL-3 isolator units.
621 Two other groups were kept together as MOCK controls in a single isolator (Supplementary
622 file 11). Throughout the experiment, the birds were fed a commercial standard diet and provided
623 with water *ad libitum*. Prior to infection (0 dpi), body weights were recorded, and blood samples
624 were taken by occipital sinus puncture. The virus used for challenge infection was A/
625 Turkey/Italy/977/1999 (kindly provided by Dr. Ilaria Capua, Istituto Zooprofilattico
626 Sperimentale Delle Venezie, Legnaro, Italy), an H7N1 subtype virus that, despite its
627 classification as an LPAIV, causes up to 50% mortality in experimentally infected White
628 Leghorn chickens [23, 58, 59].

629 Chickens were PBS/mock-treated (groups 5 and 6) or virus-infected (groups 1-4) by intra-
630 tracheal and intra-choanal cleft inoculation of 0.1mL PBS or $5x10^5$ EID^{50}/$1x10^6$ EID^{50} H7N1.
631 Animal behavior and clinical disease signs were monitored twice daily during the trial. Clinical
632 signs were evaluated according to the following score: 0 (no clinical signs), 1 (mild clinical
633 signs), 2 (severe clinical signs), or 3 (dead/euthanized). Birds were euthanized by pentobarbital
634 injection into the occipital sinus at the end of the experiment or once humane endpoints were
635 reached. Samples collected from euthanized birds included lung, caeca, and spleen. In addition,
636 a scoring system was used to evaluate macroscopic lung lesions as follows: 1 (mild, localized
637 edema and fibrinous exudate), 2 (moderate edema and with hemorrhage and fibrinous exudate
638 over ~1/4 of the lung), or 3 (severe hemorrhage and extensive edema over ~1/2 of the lung)
639 (Supplementary file 13). Data collected from the animal experiment were assessed at 2 and 6
640 dpi, which also represent the time points were the Fluidigm assay was performed. Details
641 regarding the number of birds, group distribution and number of analyzed samples are reported
642 in supplementary files 11 and 12.
643
644

645 **Quantification of the viral genome in H7N1-challenged chickens**
646 Total RNA was isolated from the isolated organs and conserved in 1ml NucleoProtect RNA
647 (Macherey-Nagel, Germany). Samples were later processed for total RNA isolation with
648 NucleoSpin RNA (Macherey-Nagel, Germany) according to the manufacturer's instructions.
649 The viral genome of the H7N1 virus was quantified using qRT-PCR that was conducted with
650 the Bio-Rad iTaq™ Universal SYBR ® Green One-Step Kit (BioRad, California, USA) using
651 primers designed for the detection of the M gene as published elsewhere [60].
652 **Histology**
653 Caeca and lungs were fixed in 10% neutral buffered formalin and processed routinely. Four-
654 micrometer tissue sections were stained with hematoxylin and eosin for light microscopy. The
655 sections' analysis addressed histopathological changes and signs of inflammatory reactions,
656 including degeneration, necrosis, infiltration of inflammatory cells, fibrin exudation, and
657 epithelial hyperplasia.
658 **Analysis of gene expression via Fluidigm Dynamic Array**
659 Gene expression was analyzed as previously described [24]. Briefly, total RNA was extracted
660 from infected animals' lungs, caeca, and spleen and processed for quality control via nanodrop.
661 Reverse transcription was performed using the High Capacity Reverse Transcription Kit
662 (Applied Biosystems) according to manufacturer's instructions with random hexamers and
663 oligo (dT)18 in a final volume of 10µl, containing 250 ng total RNA. Subsequently, the cDNA
664 was pre-amplified using TaqMan PreAmp Master Mix (Applied Biosystems). Quantitative
665 PCR was performed in the BioMark HD instrument with the 96.96 IFC Dynamic Array
666 (Fluidigm). The reaction was prepared by mixing 2.5 µl TaqMan Gene Expression Master Mix
667 (Applied Biosystems), 0.25 µl 20X DNA Binding Dye Sample Loading Reagent (Fluidigm),
668 0.25 µl 20X EvaGreen DNA binding dye (Biotum) and 2 µl of preamplified cDNA. The qPCR
669 was run under the following thermal conditions: 50°C for 2 min, 70°C for 30 min, 25°C for 10
670 min, followed by hot start 50°C for 2 min, 95°C for 10 min, PCR (x30 cycles) 95°C for 15 sec,
671 60°C for 60 sec and melting curve analysis 60°C for 3 sec to 95°C.
672 Raw quantitation cycle (Cq) data were collated with the Real-time PCR Analysis software
673 v3.1.3 (Fluidigm), setting parameters of quality Cq threshold to auto (global) and the baseline
674 correction to derivative. Raw Cq values were processed with GenEx.v6 MultiD, with correction
675 for primer efficiency and reference gene normalization. Stability of the expression of reference
676 genes: *TATA box binding protein (TBP), Tubulin alpha chain (TUBA8B), beta-actin (ACTB),*
677 *beta-glucuronidase (GUSB), glyceraldehyde-3-phosphate dehydrogenase (GAPDH) and*
678 *ribosomal 28S (r28S)* were evaluated via NormFinder (GenEx). The geometric mean of the
679 most stable (*GAPDH*, *GUSB* and *TBP*) were used for normalization. Technical replicates were

averaged, and relative quantification was to the maximum Cq value obtained per gene, transformed to logarithmic scale.

Statistical analysis

Statistical analysis was done using IBM SPSS Statistics (Version 28.0.1.1. IBM, Armonk, USA). The normality of the data was examined via Kolmogorov-Smirnov and Shapiro-Wilk tests. The comparison between two groups was made either with Two Samples T-test or Wilcoxon Signed Rank test. Multiple group comparison was made using Kruskal-Wallis Test or with One-Way ANOVA. The statistical test result was considered significant when the *P* value was less than 0.05.

Acknowledgments

Animal husbandry and experimental infrastructure was provided by the TUM Animal Research Center (ARC). The authors thank the animal keepers of the ARC as well as the team at the INRAE Plateforme d'Infectiologie Expérimentale (INRAE-PFIE, Nouzilly, France) for conducting the challenge infection experiment. In addition, we would like to thank Leah Heymelot Nabel for her help with the cloning of *RIG-I* and *RNF135*. Additionally, the authors thank the technical staff of the involved laboratories for excellent assistance.

Funding

The project was financed by a grant from the German Research Foundation to HS (DFG SI 2478/2-1). B. Schusser and TvH were supported by a grant from the German Research Foundation to BS (DFG SCHU2446/6-1). In addition, the challenge infection experiment was supported by the European infrastructure project VetBioNet (EU Horizon 2020, grant agreement No 731014). LV was supported by the Biotechnology and Biological Sciences Research Council Institute Strategic Program Grant funding (BBS/E/D/30002276).

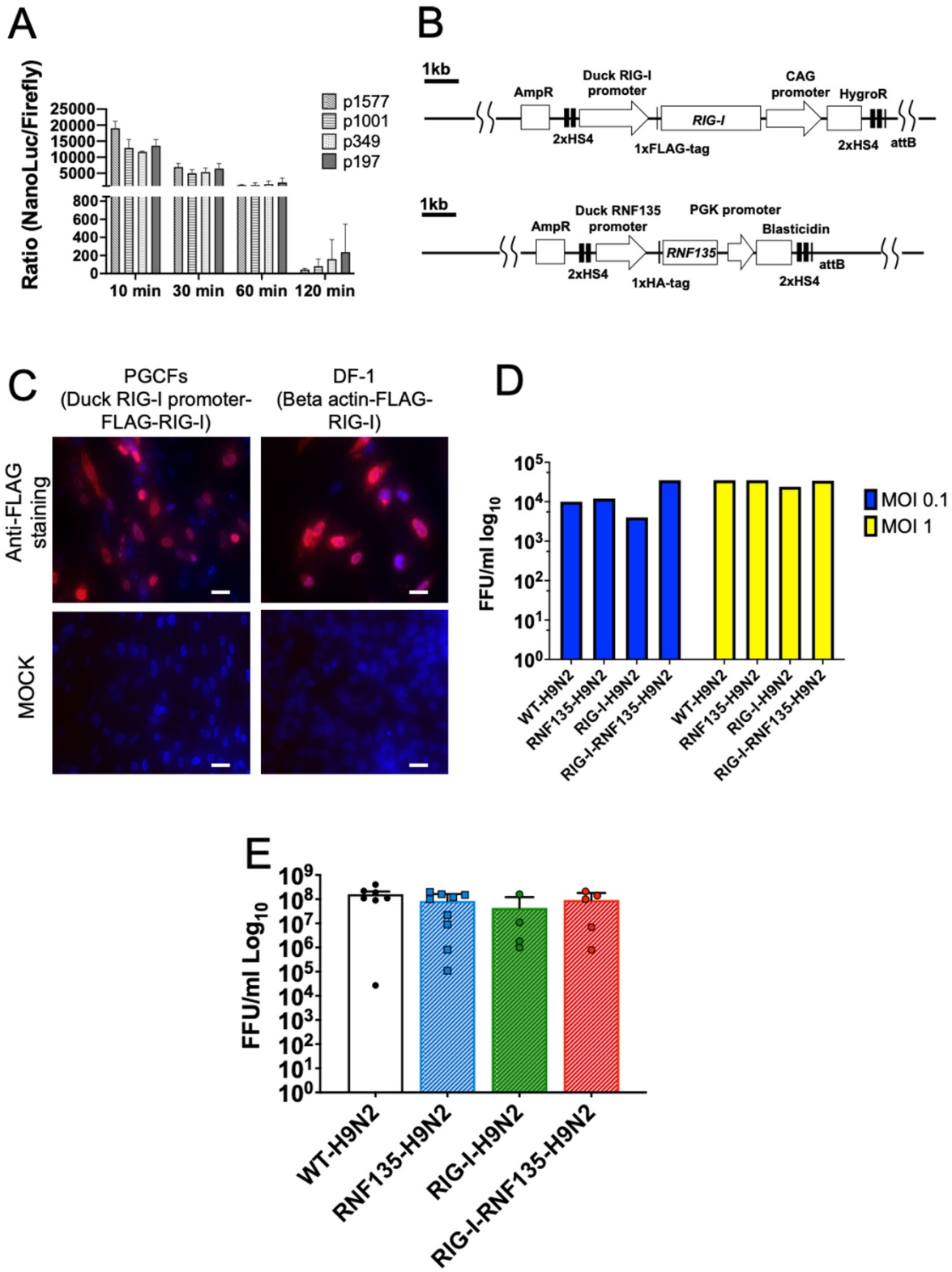

Fig. 1 Generation of PGCs, and susceptibility to infection using *in vitro* and *in vivo* systems. A. Promoter activity of the duck *RNF135* was examined by generating different deletion mutants tested in chicken DF-1 cells; the promoter activity was then evaluated by measuring the NanoLuc/Firefly ratio (n=3). B. Diagram of both constructs used to generate *RIG-I*-expressing chicken (upper diagram), using the previously identified duck *RIG-I* promoter [21] and *RNF135*-expressing chickens (lower diagram), using the duck *RNF135*

716 promoter, which activity was identified in this study. C. Primordial germ cells (PGCs) that
717 express the duck *RIG-I* under the duck *RIG-I* promoter were derived into PGC fibroblasts
718 (PGCFs) and were infected later with avian influenza virus H9N2 to stimulate *RIG-I* expression
719 upon influenza infection; the cells were infected for 18h with low pathogenic avian influenza
720 virus H9N2 and subsequently stained for FLAG-Tag; MOCK control represents uninfected
721 cells stained for anti-FLAG-Tag; DF-1 cells that express the FLAG-tagged duck *RIG-I* under
722 the chicken beta-actin promoter were used as a positive control. D. Quantification of newly
723 produced viral particles after infection of CEFs; CEFs were isolated from different transgenic
724 embryos and experimentally infected with LPAIV H9N2 at two different multiplicities of
725 infection (MOI 0.1, and 1); Supernatants were collected at 24hpi and titrated on MDCK cells;
726 no significant differences were observed between the groups (p>0.05). E. Quantification of
727 newly produced viral particles after infection of embryonated eggs. 10 day-old embryonated
728 eggs were infected with LPAIV H9N2 at 10^3 FFU/egg; allantois fluid was collected 24hpi and
729 titrated on MDCK cells; no significant differences were observed between the groups (p>0.05).
730
731
732
733

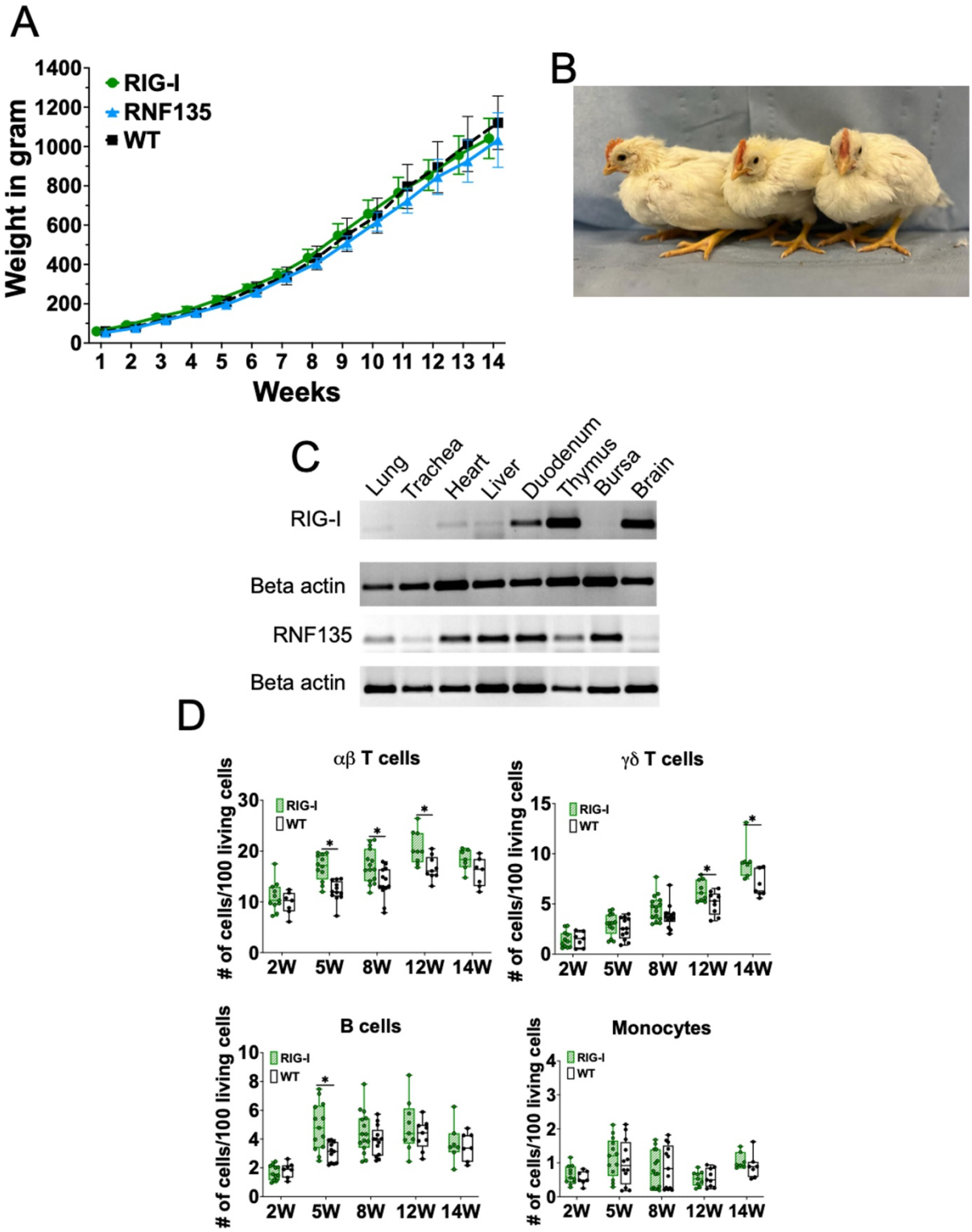

Fig. 2 Generation and immunophenotypic characterization of *RIG-I* and *RNF135*-expressing chickens. A. Weekly weight monitoring of the generated heterozygous birds (p>0.05) (n=10). B. Representative picture of the generated heterozygous birds from left to right at four weeks of age: WT, *RNF135*-expressing chicken, and *RIG-I*-expressing chicken. C. RT-PCR of the transgenic expression of *RIG-I* and *RNF135* in different organs. D. Assessment of different immune cell populations in *RIG-I*-expressing chickens compared to their WT siblings.

741
742
743

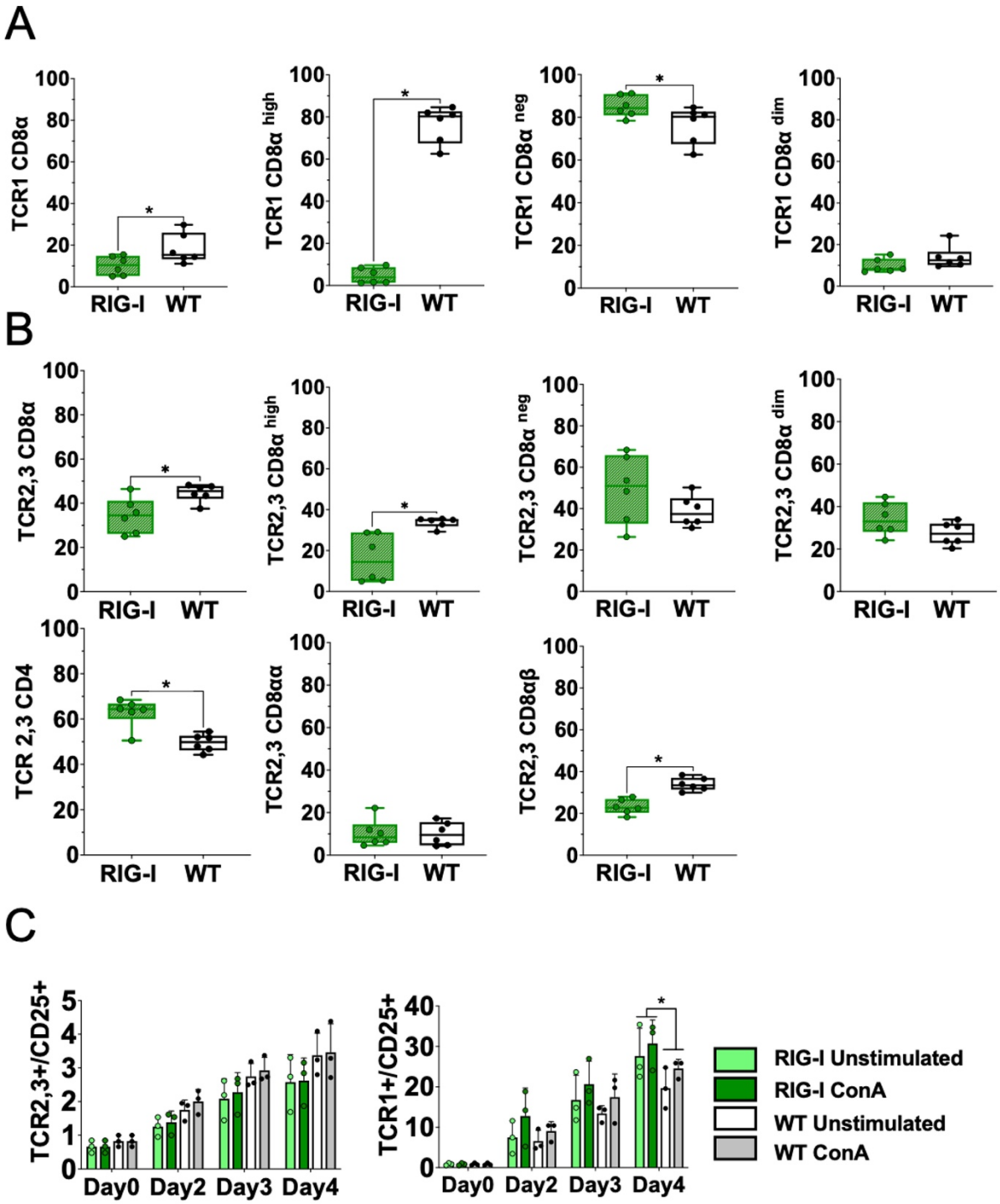

744

745 **Fig. 3 Assessment of different T cell subpopulations in *RIG-I*-expressing chickens**
746 **compared to their WT siblings**

747 A) PBMCS were analyzed for γδTCR1+/CD8α+ T cells at 12 weeks. B) PBMCS were analyzed
748 for αβTCR2,3+T cells and CD4+ or CD8α+T cells at 12 weeks ($p<0.05$). C) Activation of
749 isolated T cells from 12-week-old *RIG-I*-expressing chickens compared to their WT siblings
750 ($p<0.05$); cells were sorted according to their TCR expression, stimulated with Concanavalin

751 A, and quantified by flow cytometry at different time-points. The results indicate the number
752 of positive cells per 100 viable TCR + cells.
753
754
755
756

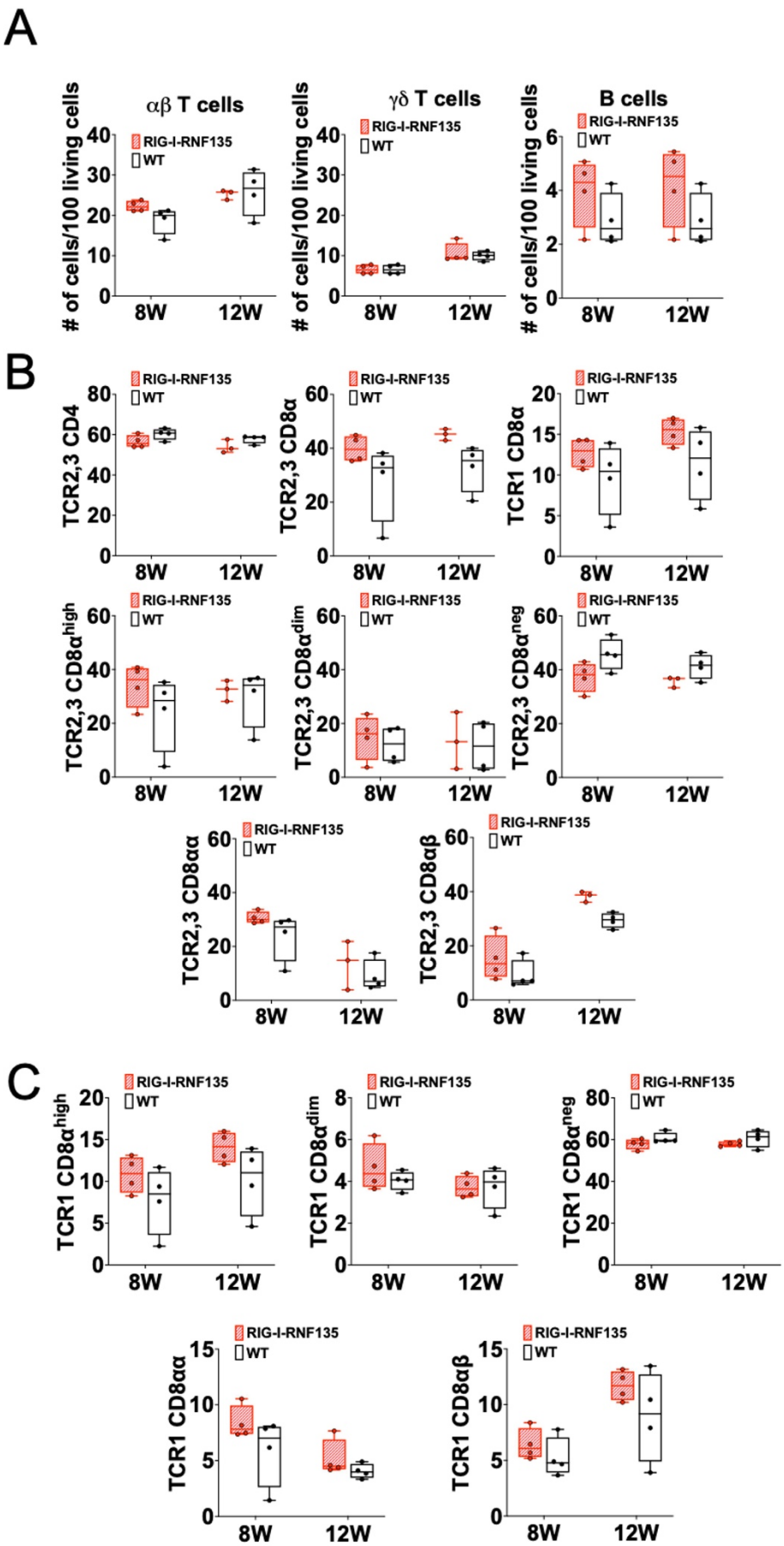
A
αβ T cells
γδ T cells
B cells
RIG-I-RNF135
WT
# of cells/100 living cells
8W
12W
B
TCR2,3 CD4
TCR2,3 CD8α
TCR1 CD8α
TCR2,3 CD8α^high
TCR2,3 CD8α^dim
TCR2,3 CD8α^neg
TCR2,3 CD8αα
TCR2,3 CD8αβ
C
TCR1 CD8α^high
TCR1 CD8α^dim
TCR1 CD8α^neg
TCR1 CD8αα
TCR1 CD8αβ

757

758 **Fig. 4 Simultaneous expression of *RIG-I* and *RNF135* in the chicken does not lead to**
759 **differences in the adaptive immune phenotype compared to WT birds**
760 Two-time points, eight and twelve weeks of age, were chosen based on the data obtained from
761 *RIG-I*-expressing chickens to assess the immunophenotype of *RIG-I-RNF135*-expressing
762 chickens. PBMCS were isolated and analyzed for B cells, αβTCR2,3+ or γδTCR1 + T cells (A)
763 as well as for CD4+ (B) and CDα8+ T cells (C). No significant differences were detected
764 between the analyzed groups ($p>0.05$).
765

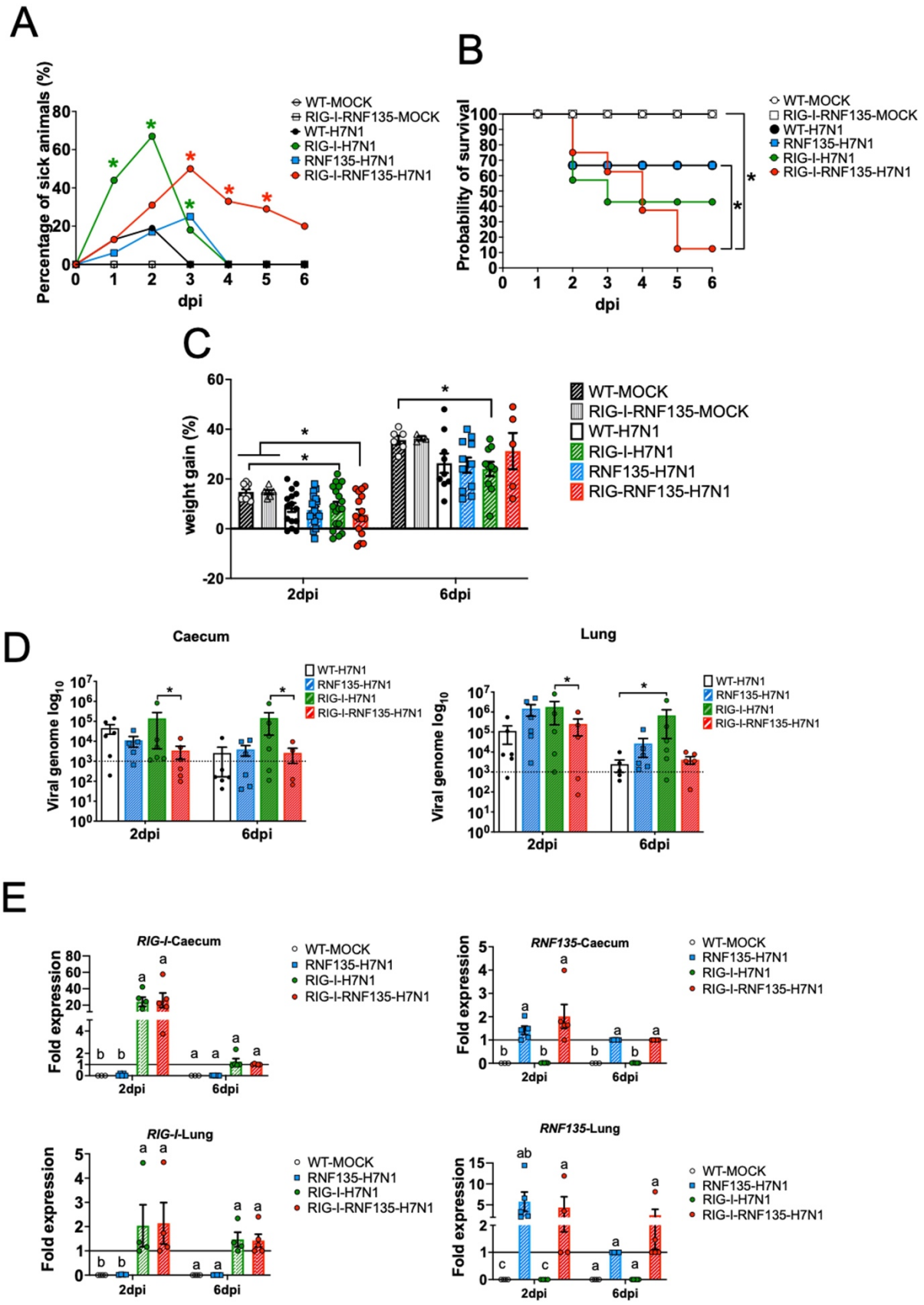
A
Percentage of sick animals (%)
dpi
WT-MOCK
RIG-I-RNF135-MOCK
WT-H7N1
RIG-I-H7N1
RNF135-H7N1
RIG-I-RNF135-H7N1
B
Probability of survival
dpi
WT-MOCK
RIG-I-RNF135-MOCK
WT-H7N1
RNF135-H7N1
RIG-I-H7N1
RIG-I-RNF135-H7N1
C
weight gain (%)
2dpi
6dpi
WT-MOCK
RIG-I-RNF135-MOCK
WT-H7N1
RIG-I-H7N1
RNF135-H7N1
RIG-RNF135-H7N1
D
Caecum
Lung
Viral genome log10
2dpi
6dpi
WT-H7N1
RNF135-H7N1
RIG-I-H7N1
RIG-I-RNF135-H7N1
E
RIG-I-Caecum
RNF135-Caecum
RIG-I-Lung
RNF135-Lung
Fold expression
2dpi
6dpi
WT-MOCK
RNF135-H7N1
RIG-I-H7N1
RIG-I-RNF135-H7N1

766

767

768

769 **Fig. 5 H7N1-challenge experiment reveals the susceptibility of *RIG-I*-expressing chickens**
770 **and the role of *RNF135* in effective *RIG-I* antiviral response.**
771 The generated transgenic chickens were challenged with H7N1 and assessed at two days post-
772 infection (dpi) and six dpi for different parameters. A) Percentage of animals presenting clinical
773 symptoms. B) Probability of survival in the challenged groups. C) Weight gain in challenged
774 groups compared to WT- and *RIG-I-RNF135*-MOCK- controls ($p<0.05$). D) Viral replication
775 rate in two main target organs, caecum, and lung ($p<0.05$); the horizontal line indicates the
776 detection threshold of the PCR based on the signal obtained from the uninfected controls, which
777 is $\log_{10}(10^3)$. E) Expression levels of transgenes in the caecum and the lung upon H7N1-
778 challenge ($p<0.05$).
779
780
781
782
783
784

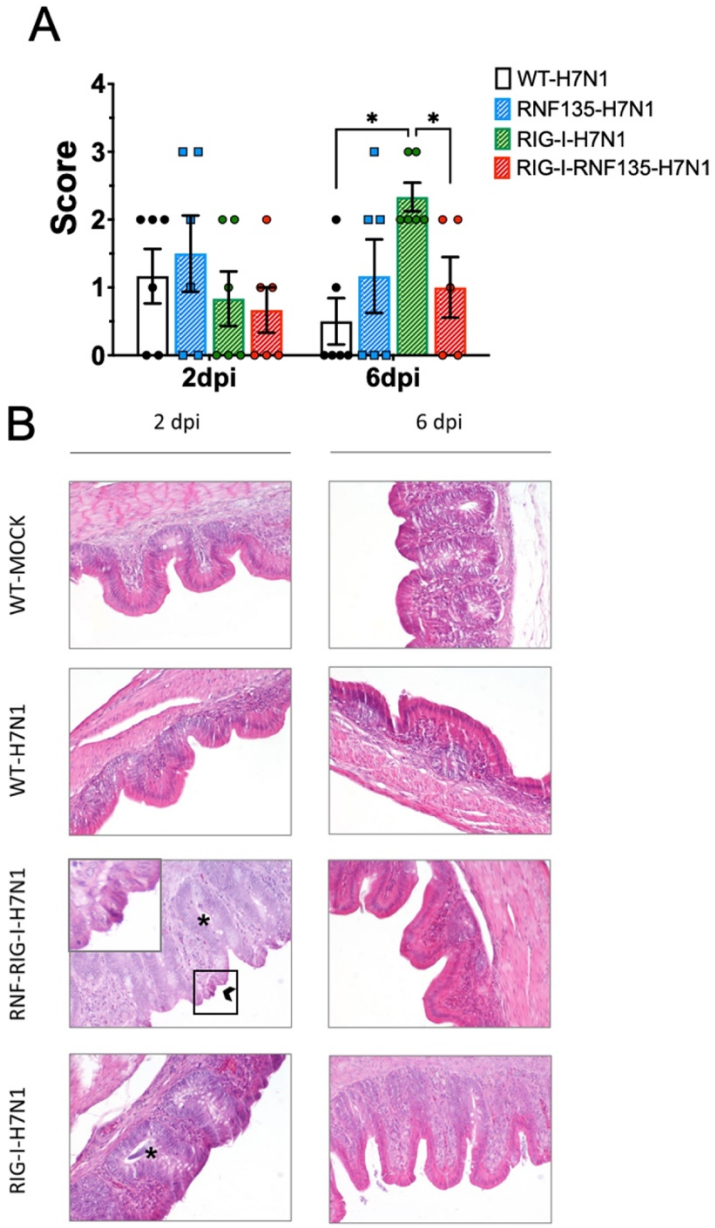

Fig. 6 Developed lesions in H7N1-challenged birds A) Macroscopical lesion score of the lungs showing significant increase of lesions in *RIG-I*-expressing birds at six dpi ($p<0.05$) B) Histology of the caecum showing the typical structure of the epithelium in the control groups. *RIG-I-RNF135* challenged birds showing epithelial hyperplasia with necrosis that diminished by 6 dpi. *RIG-I*-expressing chickens did not show necrotic lesions but pronounced epithelial hyperplasia that lessened by six dpi. Asterix indicates epithelial hyperplasia with the mitotic figures, while the arrow indicates necrotic epithelial cells; 200x.

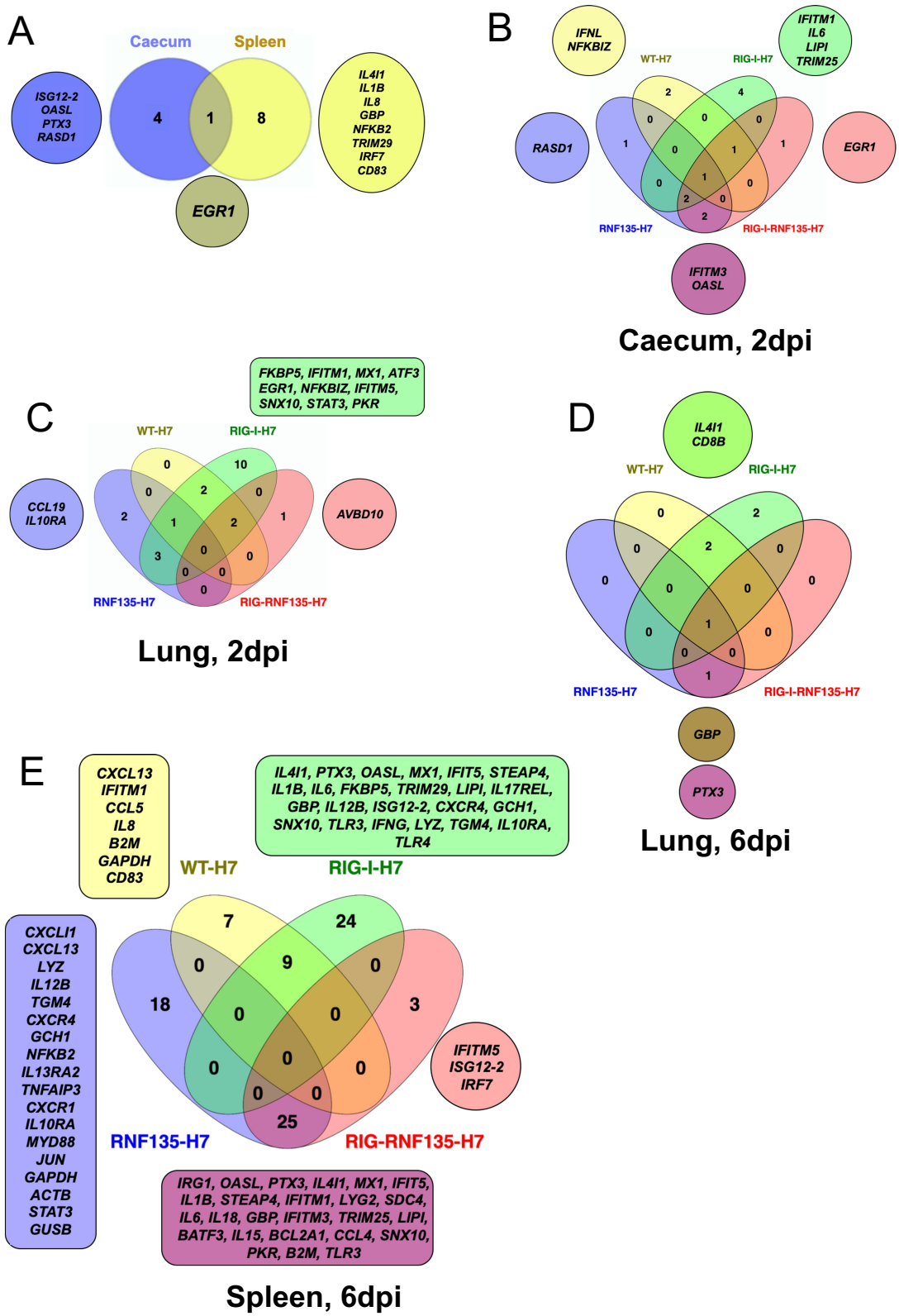

Fig. 7 Infection of transgenic chickens with H7N1 leads to upregulated inflammatory genes. Venn diagram of fluidigm qRT-PCR array of naive and challenged birds with H7N1 showing significantly upregulated genes in various organs. Significant DEGs were identified by comparing the relative expression

values for every chicken line to the WT-MOCK individually per timepoint, with a significance level set at $p < 0.05$; fold change >1 (n ≥ 5-time point).

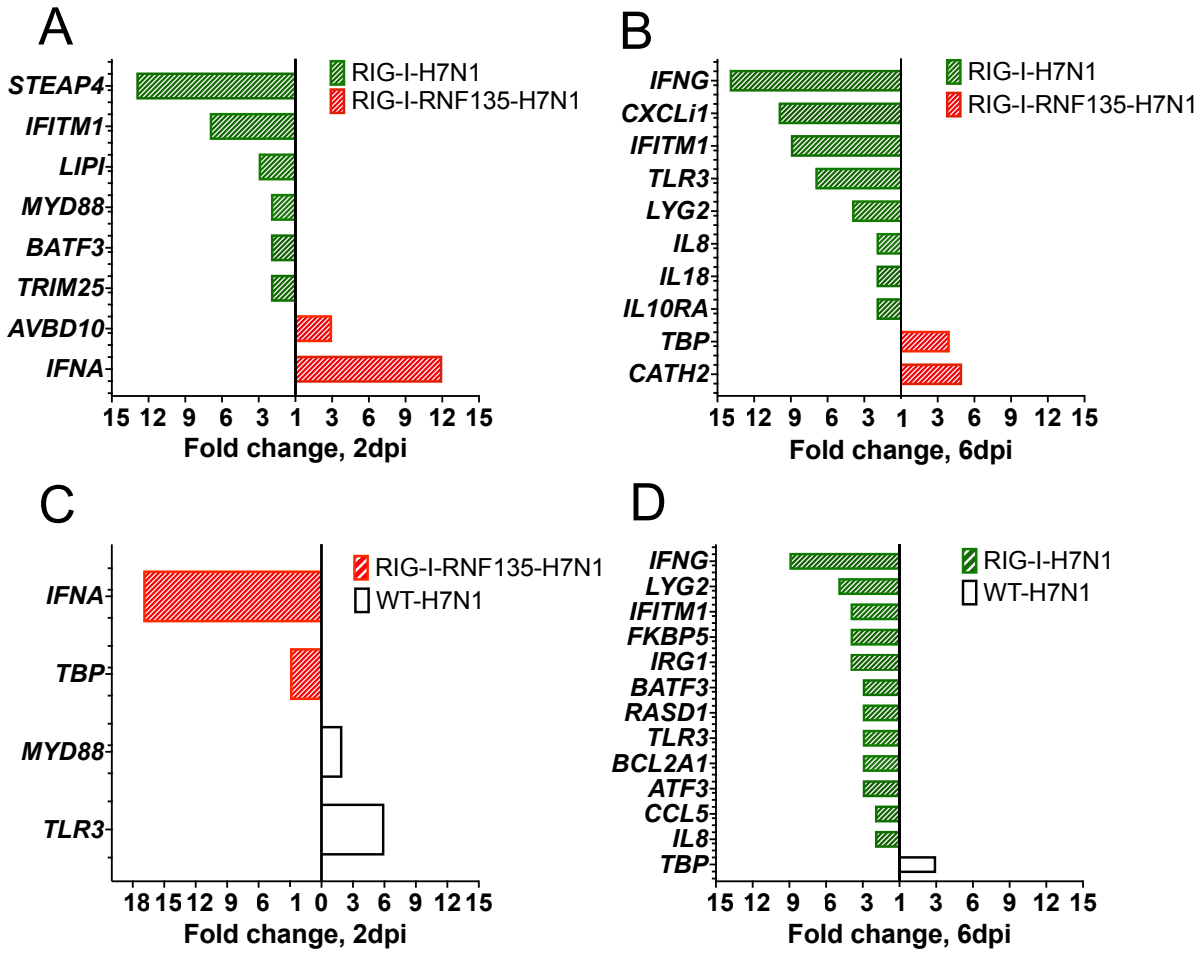

Fig. 8 Gene expression in the lung upon H7N1-infection

Significant DEGs were identified by via fluidigm qPCR array and comparison of the relative expression values between H7N1-challenged groups. A) Significantly upregulated genes after comparison of infected *RIG-I-* with *RIG-I-RNF135*-expressing chickens at two dpi. B) Significantly upregulated genes after comparison of infected *RIG-I*-with *RIG-I-RNF135*-expressing chickens at 6dpi. C) Significantly upregulated genes after comparison of infected *RIG-I-* with *RIG-I-RNF135*-expressing chickens at two dpi. D) Significantly upregulated genes after comparison of infected *RIG-I*-expressing with chickens WT-chickens at six dpi. Significance levels were set at $p < 0.05$; fold change >1 (n ≥ 5-time point).

818 **References**

819 1. Mostafa, A., Abdelwhab, E.M., Mettenleiter, T.C. & Pleschka, S. Zoonotic potential
820 of influenza A viruses: a comprehensive overview. *Viruses* **10**, 497 (2018).
821
822 2. World Health Organization. Ongoing avian influenza outbreaks in animals pose risk to
823 humans [cited 2023 July 12]. https://www.who.int/news/item/12-07-2023-ongoing-
824 avian-influenza-outbreaks-in-animals-pose-risk-to-humans.
825
826 3. MacLachlan, N. Orthomyxoviridae. *Fenner's veterinary virology*, 353-370 (2011).
827
828 4. Kim, J.K., Negovetich, N.J., Forrest, H.L. & Webster, R.G. Ducks: the "Trojan
829 horses" of H5N1 influenza. *Influenza and other respiratory viruses* **3**, 121-128 (2009).
830
831 5. Barber, M.R., Aldridge Jr, J.R., Webster, R.G. & Magor, K.E. Association of RIG-I
832 with innate immunity of ducks to influenza. *Proceedings of the National Academy of*
833 *Sciences* **107**, 5913-5918 (2010).
834
835 6. Rehwinkel, J. *et al.* RIG-I detects viral genomic RNA during negative-strand RNA
836 virus infection. *Cell* **140**, 397-408 (2010).
837
838 7. Kowalinski, E. *et al.* Structural basis for the activation of innate immune pattern-
839 recognition receptor RIG-I by viral RNA. *Cell* **147**, 423-435 (2011).
840
841 8. Yoneyama, M. *et al.* The RNA helicase RIG-I has an essential function in double-
842 stranded RNA-induced innate antiviral responses. *Nature immunology* **5**, 730-737
843 (2004).
844
845 9. Gack, M.U. *et al.* TRIM25 RING-finger E3 ubiquitin ligase is essential for RIG-I-
846 mediated antiviral activity. *Nature* **446**, 916-920 (2007).
847
848 10. Gao, D. *et al.* REUL is a novel E3 ubiquitin ligase and stimulator of retinoic-acid-
849 inducible gene-I. *PloS one* **4**, e5760 (2009).
850
851 11. Oshiumi, H. *et al.* The ubiquitin ligase Riplet is essential for RIG-I-dependent innate
852 immune responses to RNA virus infection. *Cell host & microbe* **8**, 496-509 (2010).
853
854 12. Wang, Y. *et al.* Rig-I−/− mice develop colitis associated with downregulation of Gαi2.
855 *Cell research* **17**, 858-868 (2007).
856
857 13. Pang, I.K., Pillai, P.S. & Iwasaki, A. Efficient influenza A virus replication in the
858 respiratory tract requires signals from TLR7 and RIG-I. *Proceedings of the National*
859 *Academy of Sciences* **110**, 13910-13915 (2013).
860
861 14. Cagliani, R. *et al.* RIG-I-like receptors evolved adaptively in mammals, with parallel
862 evolution at LGP2 and RIG-I. *Journal of molecular biology* **426**, 1351-1365 (2014).
863
864 15. Kandasamy, M. *et al.* RIG-I signaling is critical for efficient polyfunctional T cell
865 responses during influenza virus infection. *PLoS pathogens* **12**, e1005754 (2016).
866
867 16. Vanderven, H.A. *et al.* Avian influenza rapidly induces antiviral genes in duck lung
868 and intestine. *Molecular immunology* **51**, 316-324 (2012).
869

17. Barber, M.R., Aldridge, J.R., Jr., Webster, R.G. & Magor, K.E. Association of RIG-I with innate immunity of ducks to influenza. *Proceedings of the National Academy of Sciences of the United States of America* **107**, 5913-5918 (2010).

18. Zheng, W. & Satta, Y. Functional evolution of avian RIG-I-like receptors. *Genes* **9**, 456 (2018).

19. Krchlíková, V. *et al.* Dynamic Evolution of Avian RNA Virus Sensors: Repeated Loss of RIG-I and RIPLET. *Viruses* **15**, 3 (2022).

20. Hayman, T.J. *et al.* RIPLET, and not TRIM25, is required for endogenous RIG-I-dependent antiviral responses. *Immunology and cell biology* **97**, 840-852 (2019).

21. Xiao, Y., Reeves, M.B., Caulfield, A.F., Evseev, D. & Magor, K.E. The core promoter controls basal and inducible expression of duck retinoic acid inducible gene-I (RIG-I). *Molecular immunology* **103**, 156-165 (2018).

22. Cadena, C. *et al.* Ubiquitin-dependent and-independent roles of E3 ligase RIPLET in innate immunity. *Cell* **177**, 1187-1200. e1116 (2019).

23. Dundon, W.G., Milani, A., Cattoli, G. & Capua, I. Progressive truncation of the Non-Structural 1 gene of H7N1 avian influenza viruses following extensive circulation in poultry. *Virus research* **119**, 171-176 (2006).

24. Bryson, K.J. *et al.* Comparative Analysis of Different Inbred Chicken Lines Highlights How a Hereditary Inflammatory State Affects Susceptibility to Avian Influenza Virus. *Viruses* **15**, 591 (2023).

25. Kato, H. *et al.* Differential roles of MDA5 and RIG-I helicases in the recognition of RNA viruses. *Nature* **441**, 101-105 (2006).

26. Xu, L., Yu, D., Fan, Y., Liu, Y.-P. & Yao, Y.-G. Evolutionary selection on MDA5 and LGP2 in the chicken preserves antiviral competence in the absence of RIG-I. *Journal of Genetics and Genomics= Yi Chuan xue bao* **46**, 499-503 (2019).

27. Evseev, D., Miranzo-Navarro, D., Fleming-Canepa, X., Webster, R.G. & Magor, K.E. Avian Influenza NS1 Proteins Inhibit Human, but Not Duck, RIG-I Ubiquitination and Interferon Signaling. *Journal of Virology* **96**, e00776-00722 (2022).

28. Jiang, X. *et al.* Intrinsic RIG-I restrains STAT5 activation to modulate antitumor activity of CD8+ T cells. *The Journal of Clinical Investigation* **133** (2023).

29. Kandasamy, M. *et al.* RIG-I Signaling Is Critical for Efficient Polyfunctional T Cell Responses during Influenza Virus Infection. *PLoS pathogens* **12**, e1005754 (2016).

30. Iwamoto, A., Tsukamoto, H., Nakayama, H. & Oshiumi, H. E3 Ubiquitin Ligase Riplet Is Expressed in T Cells and Suppresses T Cell–Mediated Antitumor Immune Responses. *The Journal of Immunology* **208**, 2067-2076 (2022).

31. Elsheimer-Matulova, M. *et al.* Interleukin 4 inducible 1 gene (IL4I1) is induced in chicken phagocytes by Salmonella Enteritidis infection. *Veterinary Research* **51**, 1-8 (2020).

32. Nish, S.A. *et al.* T cell-intrinsic role of IL-6 signaling in primary and memory responses. *elife* **3**, e01949 (2014).

33. Thoresen, D.T., Galls, D., Götte, B., Wang, W. & Pyle, A.M. A rapid RIG-I signaling relay mediates efficient antiviral response. *Molecular cell* **83**, 90-104. e104 (2023).

34. Cornelissen, J., Post, J., Peeters, B., Vervelde, L. & Rebel, J. Differential innate responses of chickens and ducks to low-pathogenic avian influenza. *Avian Pathology* **41**, 519-529 (2012).

35. Liau, N.P. *et al.* The molecular basis of JAK/STAT inhibition by SOCS1. *Nature communications* **9**, 1558 (2018).

36. Palmer, D.C. & Restifo, N.P. Suppressors of cytokine signaling (SOCS) in T cell differentiation, maturation, and function. *Trends in immunology* **30**, 592-602 (2009).

37. Schmit, T. *et al.* Interferon-γ promotes monocyte-mediated lung injury during influenza infection. *Cell reports* **38** (2022).

38. Koliopoulos, M.G. *et al.* Molecular mechanism of influenza A NS1-mediated TRIM25 recognition and inhibition. *Nature communications* **9**, 1820 (2018).

39. Meyerson, N.R. *et al.* Nuclear TRIM25 specifically targets influenza virus ribonucleoproteins to block the onset of RNA chain elongation. *Cell host & microbe* **22**, 627-638. e627 (2017).

40. Okamoto, M., Kouwaki, T., Fukushima, Y. & Oshiumi, H. Regulation of RIG-I activation by K63-linked polyubiquitination. *Frontiers in immunology* **8**, 1942 (2018).

41. Woodson, C.M. & Kehn-Hall, K. Examining the role of EGR1 during viral infections. *Frontiers in Microbiology* **13**, 1020220 (2022).

42. Vazquez, C., Tan, C.Y. & Horner, S.M. Hepatitis C virus infection is inhibited by a noncanonical antiviral signaling pathway targeted by NS3-NS4A. *Journal of Virology* **93**, e00725-00719 (2019).

43. Fischer, H., Tschachler, E. & Eckhart, L. Pangolins lack IFIH1/MDA5, a cytoplasmic RNA sensor that initiates innate immune defense upon coronavirus infection. *Frontiers in immunology* **11**, 939 (2020).

44. Oshiumi, H., Matsumoto, M. & Seya, T. Ubiquitin-mediated modulation of the cytoplasmic viral RNA sensor RIG-I. *The journal of biochemistry* **151**, 5-11 (2012).

45. Chen, Y. *et al.* Duck RIG-I CARD domain induces the chicken IFN-β by activating NF-κB. *Biomed Research International* **2015** (2015).

46. Rieblinger, B. *et al.* Strong xenoprotective function by single-copy transgenes placed sequentially at a permissive locus. *Xenotransplantation* **25**, e12382 (2018).

47. Long, J.S. *et al.* Species specific differences in use of ANP32 proteins by influenza A virus. *Elife* **8**, e45066 (2019).

48. Sid, H., Hartmann, S., Winter, C. & Rautenschlein, S. Interaction of influenza A viruses with oviduct explants of different avian species. *Frontiers in Microbiology* **8**, 1338 (2017).

49. Van de Lavoir, M.-C. *et al.* Interspecific germline transmission of cultured primordial germ cells. *PLoS One* **7**, e35664 (2012).

50. Van de Lavoir, M.-C. *et al.* Germline transmission of genetically modified primordial germ cells. *Nature* **441**, 766-769 (2006).

51. Leighton, P.A., van de Lavoir, M.C., Diamond, J.H., Xia, C. & Etches, R.J. Genetic modification of primordial germ cells by gene trapping, gene targeting, and ϕC31 integrase. *Molecular Reproduction and Development: Incorporating Gamete Research* **75**, 1163-1175 (2008).

52. Hamburger, V. & Hamilton, H.L. A series of normal stages in the development of the chick embryo. *Journal of morphology* **88**, 49-92 (1951).

53. Whyte, J. *et al.* FGF, insulin, and SMAD signaling cooperate for avian primordial germ cell self-renewal. *Stem cell reports* **5**, 1171-1182 (2015).

54. Schusser, B. *et al.* Immunoglobulin knockout chickens via efficient homologous recombination in primordial germ cells. *Proceedings of the National Academy of Sciences* **110**, 20170-20175 (2013).

55. Hernandez, R. & Brown, D.T. Growth and maintenance of chick embryo fibroblasts (CEF). *Current protocols in microbiology* **17**, A. 4I. 1-A. 4I. 8 (2010).

56. Brauer, R. & Chen, P. Influenza virus propagation in embryonated chicken eggs. *JoVE (Journal of Visualized Experiments)*, e52421 (2015).

57. Kong, F.-k., Chen, C.-l.H., Six, A., Hockett, R.D. & Cooper, M.D. T cell receptor gene deletion circles identify recent thymic emigrants in the peripheral T cell pool. *Proceedings of the National Academy of Sciences* **96**, 1536-1540 (1999).

58. Monne, I. *et al.* Emergence of a highly pathogenic avian influenza virus from a low-pathogenic progenitor. *Journal of virology* **88**, 4375-4388 (2014).

59. Trapp, S. *et al.* Major contribution of the RNA-binding domain of NS1 in the pathogenicity and replication potential of an avian H7N1 influenza virus in chickens. *Virology journal* **15**, 1-12 (2018).

60. Ward, C. *et al.* Design and performance testing of quantitative real time PCR assays for influenza A and B viral load measurement. *Journal of clinical virology* **29**, 179-188 (2004).

1027 **Supplementary Data**

1028

1029 **Supplementary file 1: Immunophenotype of *RNF135*-expressing chickens**

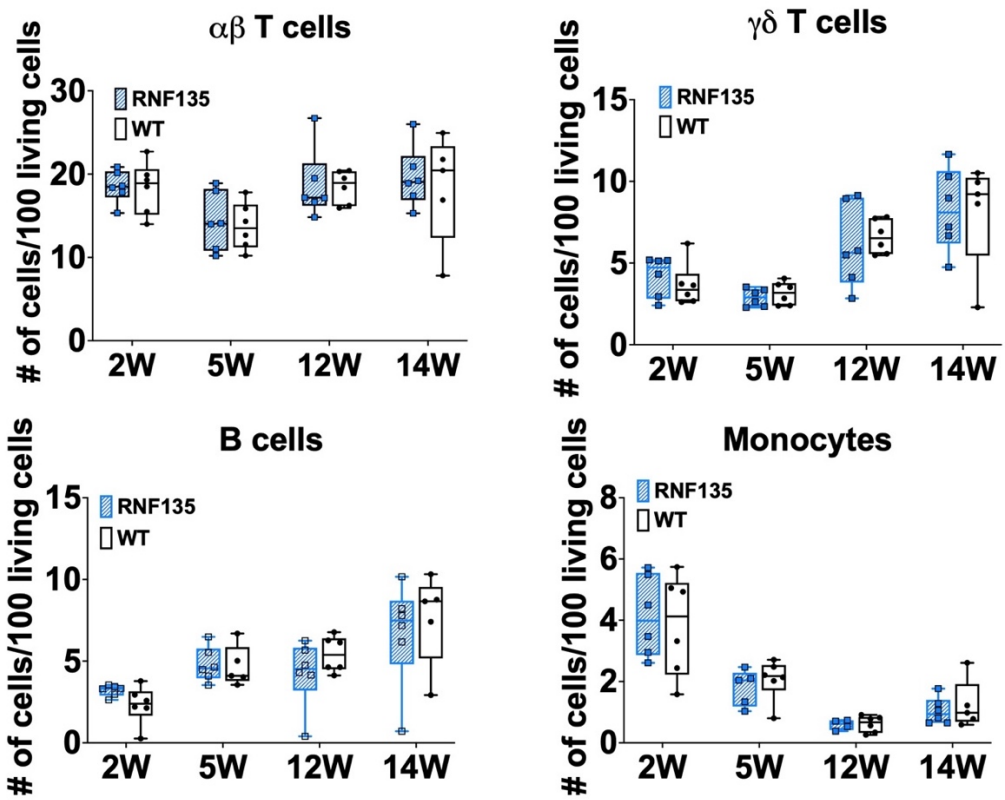

1030

1031

1032

1033

1034

1035

1036

1037

1038

1039

1040

1041

Supplementary file 2: Immunoglobulin levels in *RIG-I*-expressing birds compared to WT
Relative amounts of total plasma IgM and IgY in *RIG-I*-expressing birds and their WT siblings compared by ELISA at 12 weeks of age (n≥3)

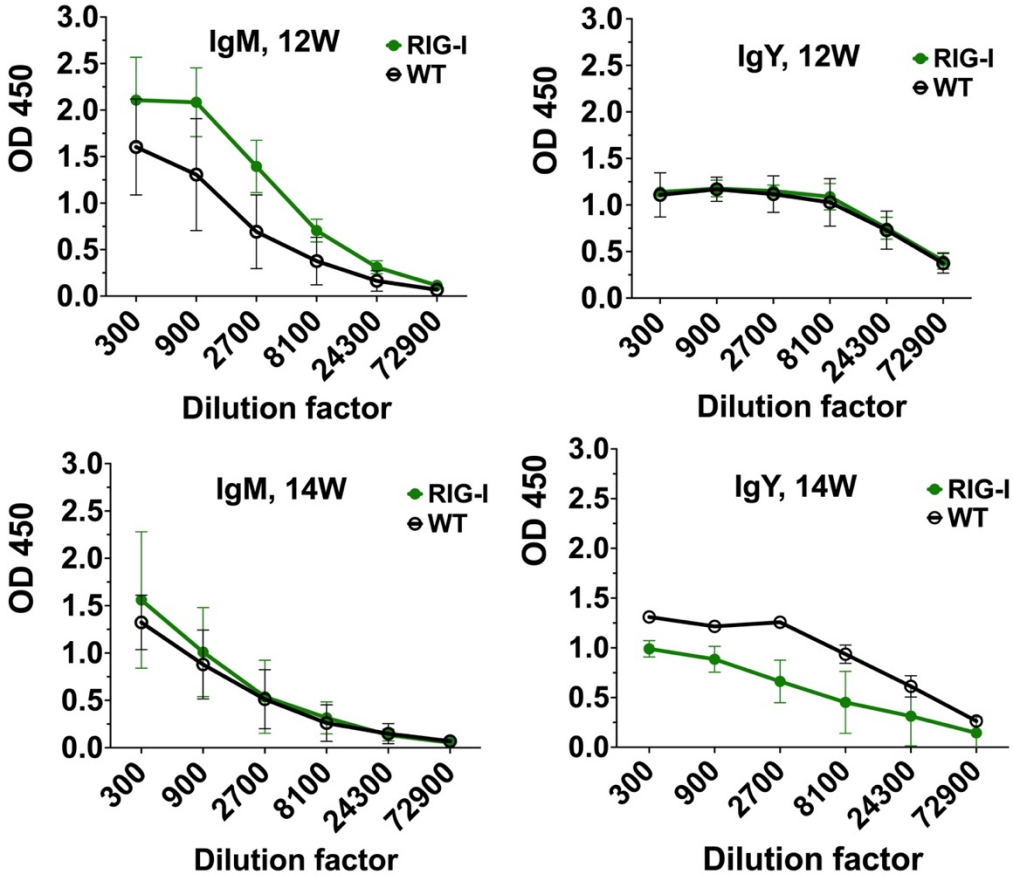

1068 **Supplementary file 3: Body weight development over 14 weeks of *RIG-I-RNF135*-**
1069 **expressing chickens in comparison to WT siblings (n ≥4)**
1070

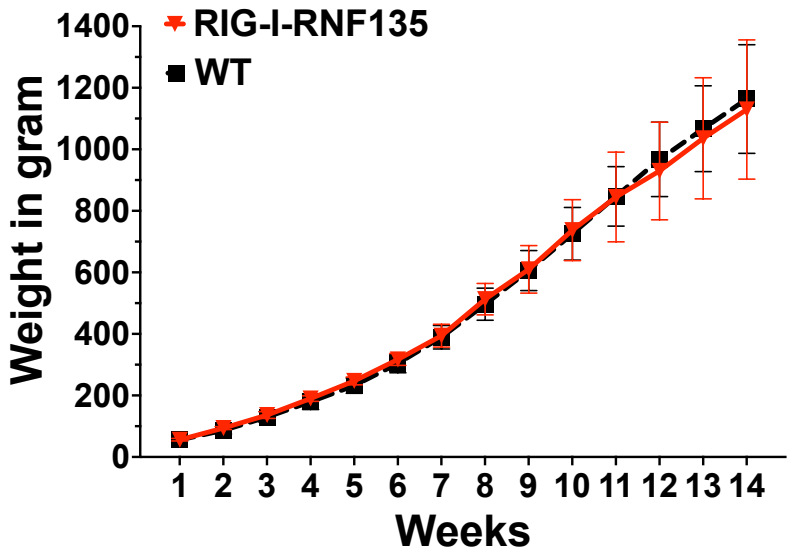

1071

1072
1073
1074
1075
1076
1077
1078
1079
1080
1081
1082
1083
1084
1085
1086
1087
1088
1089
1090
1091
1092
1093
1094
1095
1096
1097
1098
1099
1100

Supplementary file 4: Fluidigm qRT-PCR array of naive and challenged birds with H7N1 A) Principal component analysis (PCA) of global gene expression of viral innate immune-related genes. B) *RIG-I-RNF135* MOCK compared to WT-MOCK birds; positive values indicate high expression in the *RIG-I-RNF135* expressing chickens, while negative values indicate high expression in WT-MOCK. C) Expressed genes in the caecum of infected groups compared to WT-MOCK at 2dpi; positive values indicate high expression in the infected groups (1=WT-H7N1, 2=*RIG-I-RNF135*-H7N1, 3=*RIG-I*-H7N1, 4=*RNF135*-H7N1), while negative values indicate high expression in WT-MOCK. Significant DEGs were identified by comparing the relative expression values for every chicken line to the WT-MOCK individually per timepoint, with a significance level set at $p < 0.05$; fold change >1 (n ≥5/timepoint)

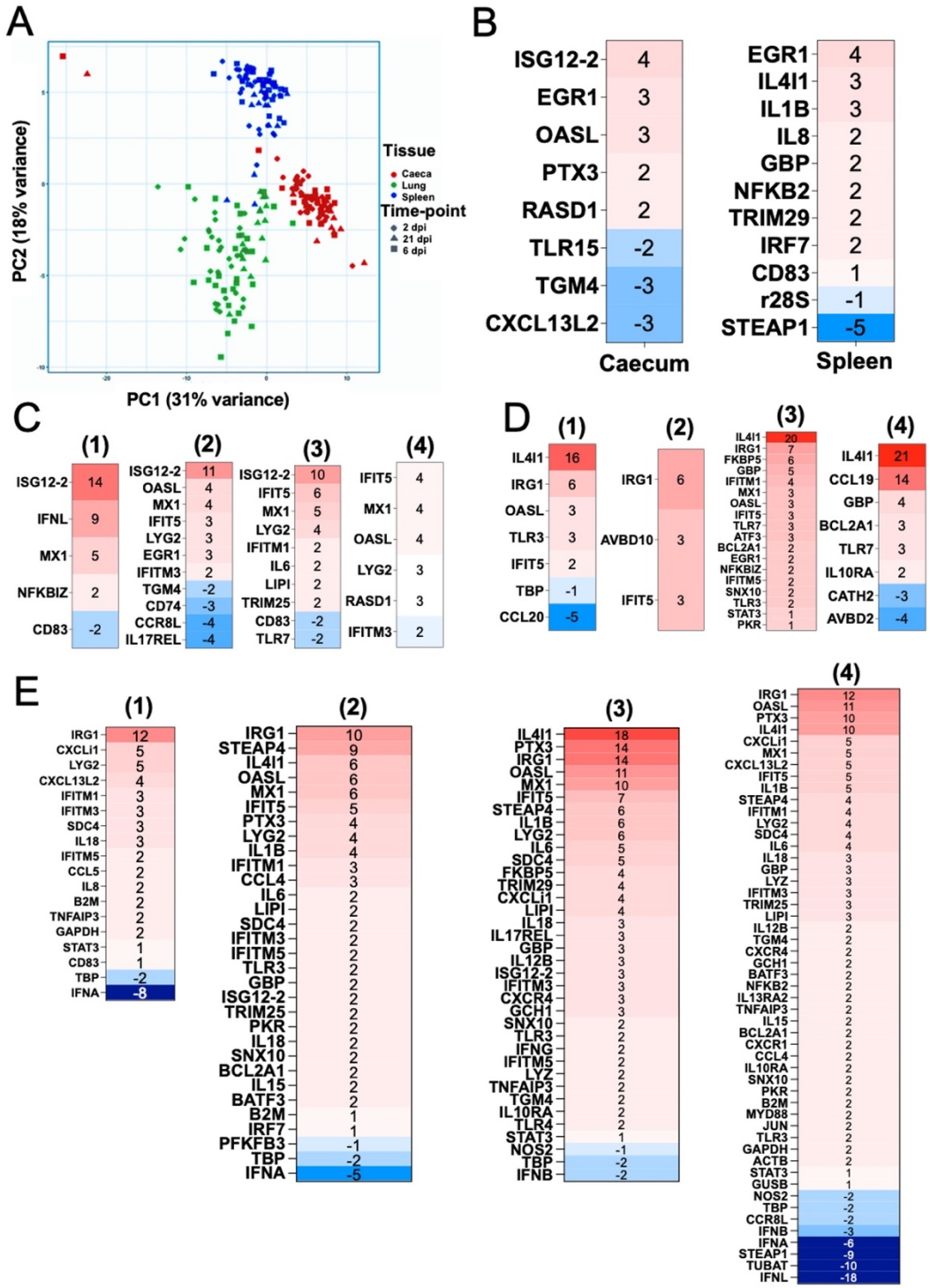

Supplementary file 5: Involvement of the regulated genes in the biological processes. Each category is represented by a different color (Biological Process = red , Cellular Component = blue and Molecular Function = green). A) regulated genes in the caecum and spleen of *RIG-I-RNF135*-expresing birds. The height of the bar represents the number of IDs in the uploaded list of genes and the category. B) Function of genes expressed in the lung and caecum of *RIG-I*-expressing chickens C) Function of genes expressed in the spleen of *RIG-I*-expressing chickens at 6dpi. Figures were generated using WebGestalt (WEB-based GEne SeT AnaLysis Toolkit).

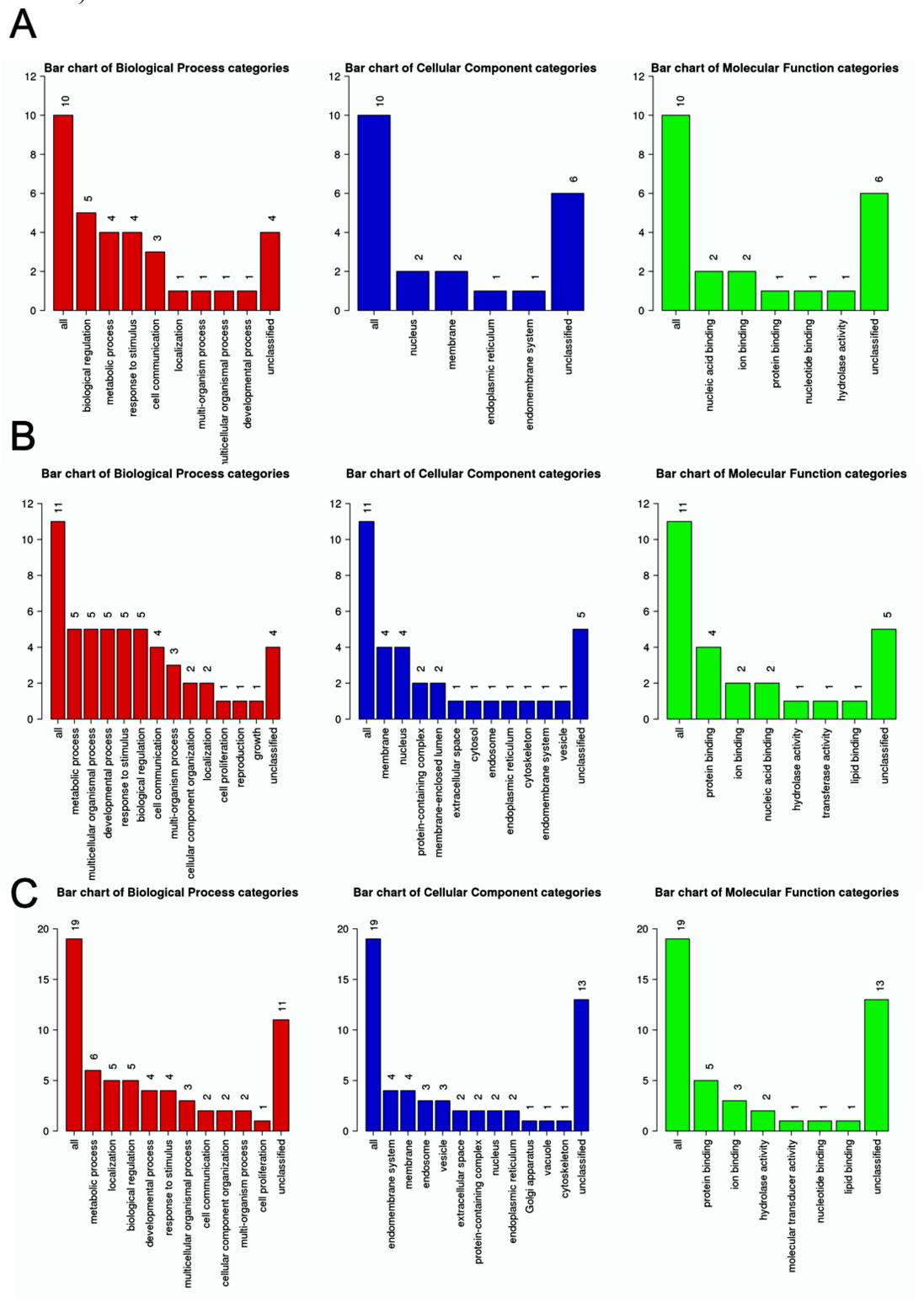

Supplementary file 6: Sequence of duck *RNF135* promoter and the duck *RNF135*

Duck RNF135 promoter (*Anas platyrhynchos*)

GGAGCAGAGCCAGGCAGCTATAGTCTACCTGACTGCAGCTCCTATCCAGACAGGGACATGTTTCTTTTCCATGGAGTGGTTTTAATGCCTTTTACAGTGTTAGATTTCTG
TCACAGAAATTGTAAAAAAAATAAAAGTCAAGTTTGAATTGTGGAGAATACTGTAATGGAATCACTCTAATGACAGATGTCCCTACCTCCTTGCTTTCAACAGTCTCTGCTA
TTTGATTCTTTTATGAGTGGCAAATGAGACATGTAAAGACTTTTTTTTTCTTTTCCAAAGCAACCCCCACATACTGCCTCAGTCAAGACGAGTTCATGATGAAGACACACTG
ATTGGTATTACCTCCTAAAAACAGCTAAAGCTTTGGGTCATGAGTTCACTTACTGAATTTGAGTAGTCTGAGCAGTGAAAGGCAGAAGTCAGTTTTAAAAGTGCTGTCTTC
CTTGGCTTGTTTGAAGACACTCAATGTATGAGGACCAGCACGGAAAGCACAGAGTGAGTGCCTCCTGATCAGGTGCTACGTACATCCATTCTGCGCAGGAATGGGTGA
GGATTTGCACTGGCTCACAAAGGGCACTGAGTGTTTTCTTGCCTCACAGCCAAGCCCAAGATTTGGTTCTACCAAGAAGTCAGTCATTCAGATATTTAATTCTTCTTTTCA
GATTCCCTTAGTTTGCAAATCAAGCGGAAGTCTTGCAAACTAAGCTTCTGGTAAAGCTTCCACCTTTTGCTGTTGCTTGCCAGCCAGTCTAAGGCACCCCAAATAGTTCTA
CAGAAAGAAGGAAGTACCAATATATGCAGGGATTAGTGTGATTAACTCTTTTTTTCCCACAACAGTACAGAAAATTTGACTTGGTTCATCATTCTGTCTGTCTTAGTCAACT
CATCATCTTCCAGCCTTGAACAAACTGCAGGAGTTTTGCTTCCTGACATTCTCCCATAAACTCCCTGATGTTTCTGTTCTTTCTTTCCTCTCCCCATACGATCTGGGGAATT
ACAGTTCACGTGCTGGTTCAGCAAATCTTGTAACAGCCTCATCCTGCAGCTCCTGAAATCAACAGCGAGGCACTTGTTGAAGATCATAGTCTGGTTTGAGATGCTTTTTT
TTATTATTTATTTTGAGGTGAGCTGAGCAATTCTGGATGATCTCAAAAAGTTTAGTCTACTCAGAAGCCTCAGCTTCACGGATGGGGTTCCCTGTGTGATGTCCGGGAAA
GGTCAGCAGACCAACCGTGTCAGCAACCCTGTTACAAAACCAGGAAATTCCCAGAAGAAAAAAAAAAAATGCTACTGTGCGAAGACGACAACTTTTTGCAGACTGGAGGC
GAGGTTACGGAGAGCTCCGTGTGACGGTACCTTCCTACAGCCAACCCAAGTCCTGGCGCCGAGCTGAAGGCAGCAGCAGCACCGGAGCCCGGCTTCGCGGGTGCCC
CGGGCCTTCAGCTGCCGGTAGCCCCGCACCGGGCCCGGTCCAGCACCGAGCCCAGCCCCACACCGGGCCCGGCCCCCCCGGCGGGAGGCGGCGCCCCGAGGAAA
CGAAACCGCGCCGCGCTCCGCTCCGCCCCGAGCAGGACCT

GC-optimised duck RNF135 sequence (*Anas platyrhynchos*)

ATGTATCCTTATGATGTTCCCGATTATGCTGCGGTTCCCGCTGAGCTTGGCCGGCTCCTCGCTGACGTTGAACTCAGCTGTTCATGCTGTTTGCAGTACTTTACCGAGCC
CGTACGGTTGGCGTCTTGCTCTCACAGCTTCTGTCGGAGCTGTATCGACACGTACTGTCGGGGTCGCCGGCGGGCACCCTGCCCTCTCTGCAGAGAGGATTTTGAGC
CGAAAGATTTGCGCCCGAATAGAGAACTTGCAGCCCTTGTCTCACTCATGTTGGGCGGAGGCAGAGGTGAGGGACTGGGTGCATGGGATCAACCGACAGCATCTGGT
GACGGGGCGGGCGGAGGGTGCAGCAGTGCCTGGAGACGCCCGGGGGAAAAGGAGGAGCAAATACGGGATATTAGCAAACAGCTTGAGATAACTAAGGAAACTATTA
ATGCGCTGCGGAAAGATTTGTCTAAGACGAAAGAATATACAAGCCAAATACTCTCACAAATAACAGAGGACTTTTGCTGCATGAAAGAGTATATTGAGAGGCAAGAAGAA
AATACTTTGATGTTCATCGAACAGGAACAGAGGGCGGCCCGGCAAAAGATAGTACAAACTATCCACCAGCTTTGTGTTGAAAAATACAAATTGATAGACATAAAGGCGCA
AATGGAGAAGGGGTTGGAAAGTGACGAAATGGAATGGCAGACCTCTAACCTTCTTGAGAGAGGTGGAGGGAGCCCTAGTACCATGCATAAGTTCACAATCGATGAGAA
ATTCAACGTCGTTAGGAGCGCCGTAGGAGATCTGAAAAGAAAATTGGAGATCTTGCTGCTCGAAGAGTATCCTCAACAATTCCCACCAGCCCAAAGTCCCGACTTGCAT
CAGGAAACGAGTGTCTGTTCATTGTCATCCGAAAGCGCGGCTAAGTCACCCGAACCGTCTATCTCATCCCAATTTTCACGCTGGGCTGATAACGTCACCTTTGACTTGAC
GACCGCCTATGATAGACTTGCCATCACCGATCAGAATAGAAAAGTTATGGTGTCATCTAACCCAACCTATTACGAGCCATCCCTTAAACGGTTCTGTATAAGTCAGGTTCT
TTGCAGCCAAGGCTTCAGTACCGGGTGCCACTATTGGGAGGTAATCACCAAGGACAGCGACGGTTGGGCGGTTGGCGTTGCCAGAGGAACCATCGGGAGACGGGAT
CGCTTGGGACGGACCGAGTCAAGTTGGTGTGTGGAGTGGGTGGGACCTCAGAAGCAGCTGAGCGCCTGGCATCGCAATCAAGAGACACTGCTGCGGAACGACAAGC
CACTTAAAGTAGGCGTGTTCCTTGAACTGCAAAAGACCGTATCTTTTTATGCGATAACCGATCGCGAGATGCTCTTGCATACATTCGAAATCAATAACAGTAACCCTTTGT
ACCCGGCCTTCTGGCTCTATAGCTTGGACAAGAACGGCTCTCTTACGATAAATCATATTAACAGGAAATAAG

Protein sequence of the duck RNF135 (*Anas platyrhynchos*)

M**YPYDVPDYAA**VPAELGRLLADVELSCSCCLQYFTEPVRLASCSHSFCRSCIDTYCRGRRRAPCPLCREDFEPKDLRPNRELAALVSLMLGGGRGEGLGAWDQPTASGDGA
GGGCSSAWRRPGEKEEQIRDISKQLEITKETINALRKDLSKTKEYTSQILSQITEDFCCMKEYIERQEENTLMFIEQEQRAARQKIVQTIHQLCVEKYKLIDIKAQMEKGLESDEME
WQTSNLLERGGGSPSTMHKFTIDEKFNVVRSAVGDLKRKLEILLLEEYPQQFPPAQSPDLHQETSVCSLSSESAAKSPEPSISSQFSRWADNVTFDLTTAYDRLAITDQNRKVM
VSSNPTYYEPSLKRFCISQVLCSQGFSTGCHYWEVITKDSDGWAVGVARGTIGRRDRLGRTESSWCVEWVGPQKQLSAWHRNQETLLRNDKPLKVGVFLELQKTVSFYAITD
REMLLHTFEINNSNPLYPAFWLYSLDKNGSLTINHINRK*

Blue colored letters indicate the inserted HA tag

Supplementary file 7: Results of Droplet Digital PCR (ddPCR) of PGCs that express the duck *RIG-I* (A) and those who express the duck *RNF135* (B)

A) #253 indicates the construct with the full *RIG-I* length promoter used to express the duck *RNF135* in PGCs. Clone #1 was used for the generation of *RIG-I* chimeric roosters.

B) #258 indicates the construct number used to express the duck *RNF135* in PGCs. Clone #6 was used for the generation of *RNF135* chimeric roosters.

C) Selected clones were derived into fibroblasts (PGC-derived fibroblasts) and tested for the *RIG-I* activity by the detection of FLAG-Tag

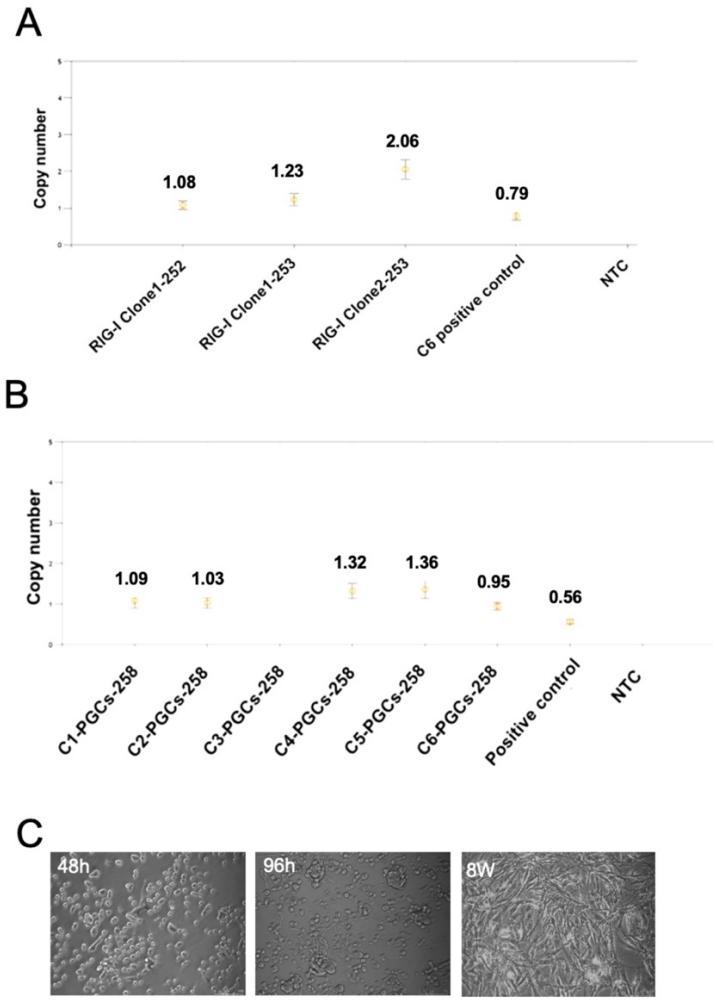

1164 **Supplementary file 8: clones and concentrations of used antibodies**

Antibody	Company	Clone	Assay	Concentration
Mouse Anti-Chicken TCRγδ-UNLB	Biozol	TCR1	Flow cytometry	0.625 µg/mL
mouse anti-chicken TCRαβ/Vb1-UNLB	Biozol	TCR2	Flow cytometry	2.5µg/mL
mouse anti-chicken TCRαβ/Vb2-UNLB	Biozol	TCR3	Flow cytometry	2.5µg/mL
mouse-IgG1_anti-chicken chB6_UNLAB	Biozol	AV20	Flow cytometry	2.5µg/mL
mouse IgG2a -anti-chicken KUL01_UNLAB	Biozol	KUL01	Flow cytometry	0.625 µg/mL
goat anti-mouse IgG (H+L)-APC	Biozol	Polyclonal	Flow cytometry	0.625 µg/mL
mouse-IgG1_anti-chicken CD8α_PacBlue	Biozol	CT-8	Flow cytometry	0.625 µg/mL
mouse IgG2a -anti-chicken CD8ß_UNLAB	Biozol	EP42	Flow cytometry	0.625 µg/mL
mouse IgG1-anti-chicken CD4_FITC	Biozol	CT-4	Flow cytometry	0.625 µg/mL
mouse IgG1 Anti-Chicken TCRγδ-BIOT	Biozol	TCR-1	Flow cytometry	0.625 µg/mL
mouse anti-chicken TCRαβ/Vb1-BIOT	Biozol	TCR-2	Flow cytometry	2.5µg/mL
mouse anti-chicken TCRαβ/Vb2-BIOT	Biozol	TCR-3	Flow cytometry	2.5µg/mL
mouse anti-chicken Bu1-FITC	Biozol	AV-20	Flow cytometry	2.5µg/mL
mouse anti- chicken MRC1L-B	Biozol	KUL01	Flow cytometry	0.625 µg/mL
rat-anti-mouse IgG2a_PE	Biozol	SB84a	Flow cytometry	0.125µg/mL
Streptavidin_APC	VWR	-	Flow cytometry	0.2µg/mL
goat anti-mouse IgG (H+L)-APC	Biozol	polyclonal	Flow cytometery	0.625 µg/mL
Human anti-Chicken CD25	Biorad	monoclonal	Flow cytometery (T cell activation)	2.5µg/mL
Fixable Viability Dye eFluor 780	eBioscience		Flow cytometery	1:1000
Goat anti-chicken IgM	Biomol	polyclonal	ELISA	2µg/mL
Rabbit anti-chicken IgY (used for coating ELISA plates)	Jackson	polyclonal	ELISA	2µg/mL
Goat anti-chicken IgM-HRP	Biomol	polyclonal	ELISA	0.05ng/mL
Rabbit Anti-Chicken IgY-HRP (used for detection)	Jackson	polyclonal	ELISA	0.02µg/mL

1165

1166 **Supplementary file 9: Germline transmission of the injected PGC clones**

Injected PGC clone	Germline transmission (%)
RIG-I	10.2
RNF135	6

1167

1168

1169

1170

1171

1172

1173

1174

1175

1176

1177

1178

1179

1180

1181

1182

1183

1184

1185

1186

1187

1188

Supplementary file 10 Gating strategies for the detection of different immune cells. A) Detection of B cells and monocytes. B) detection of T cell subpopulations. C)Live/Dead staining and detection of TCRαβ1, αβ2/CD25+ T cells and TCRγδ/CD25+ T cells

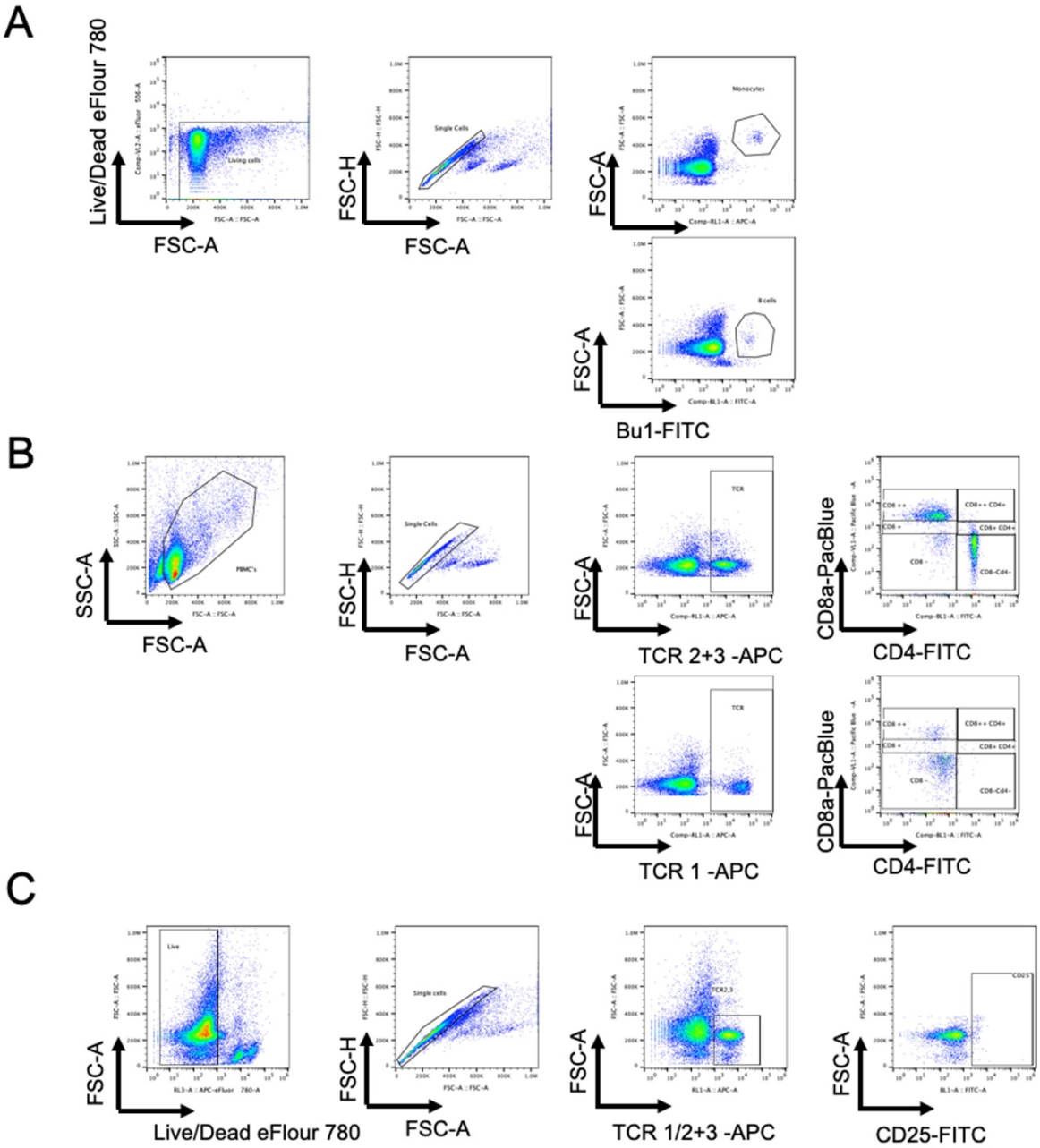

1202 **Supplementary file 11: Group distribution and number of birds used in the**
1203 **experimental challenge with H7N1**

Genotype	**RIG-I-RNF135**		**WT**		**RIG-I**		**RNF135**		**WT**		**RIG-I-RNF135**	
Inoculation	**H7N1**		**H7N1**		**H7N1**		**H7N1**		**MOCK**		**MOCK**	
Number	**(n=16)**		**(n=16)**		**(n=18)**		**(n=18)**		**(n=9)**		**(n=6)**	
animal # (sex)	204	male	201	female	202	male	205	male	210	male	242	male
animal # (sex)	206	female	209	male	208	female	216	female	233	male	248	female
animal # (sex)	213	male	214	female	211	male	220	male	252	female	260	male
animal # (sex)	227	male	215	female	218	male	235	female	255	male	268	female
animal # (sex)	222	female	226	male	225	male	239	female	264	female	276	female
animal # (sex)	238	male	228	male	230	female	257	male	270	female	311	male
animal # (sex)	246	female	234	female	231	female	273	male	288	female		
animal # (sex)	253	female	237	female	232	female	274	female	298	male		
animal # (sex)	258	female	243	male	240	male	277	male	290	female		
animal # (sex)	262	male	267	female	244	female	279	female				
animal # (sex)	271	male	284	male	247	female	285	female				
animal # (sex)	278	female	301	female	249	male	286	female				
animal # (sex)	280	female	302	female	259	female	287	male				
animal # (sex)	282	male	303	male	265	male	292	female				
animal # (sex)	291	female	306	male	275	female	295	male				
animal # (sex)	294	female	317	male	281	female	307	male				
animal # (sex)					283	male	310	female				
animal # (sex)					305	male	322	male				

1204

1205
1206
1207
1208
1209
1210
1211
1212
1213
1214
1215
1216
1217
1218
1219
1220
1221
1222
1223
1224
1225
1226
1227
1228
1229

1230 **Supplementary file 12: Number of sampled birds for organs at different days post-**
1231 **infection (dpi)**

Group	Number of sampled birds		
	2dpi	**6dpi**	**21dpi**
RIG-I-RNF135-H7N1	6	5	0
WT-H7N1	7	6	3
RIG-I-H7N1	7	6	4
RNF135-H7N1	6	6	6
WT-MOCK	3	3	3
RIG-I-RNF135-MOCK	3	3	0

1232
1233
1234
1235
1236
1237
1238
1239
1240
1241
1242
1243
1244
1245
1246
1247
1248
1249
1250
1251
1252
1253

1254 **Supplementary file 13: Score system used to evaluate influenza-induced lung lesions.**

1255

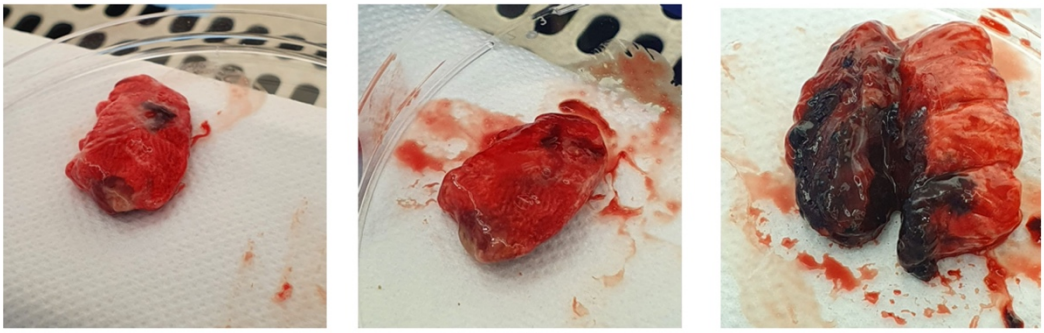

Score 1 (+)
Mild, localized edema and fibrinous exudate

Score 2 (++)
Moderate edema with hemorrhage and fibrinous exudate over about 1/4 of the lung

Score 3 (+++)
Severe hemorrhage and extensive edema over about 1/2 of the lung

1256

1257

1258

1259

1260

1261

1262

1263

1264

1265

1266

1267

1268

1269

1270

1271

1272

1273